NASA Technical Memorandum 4200

Static Wind-Tunnel and Radio-Controlled Flight Test Investigation of a Remotely Piloted Vehicle Having a Delta Wing Planform

Long P. Yip, David J. Fratello,
David B. Robelen, and George M. Makowiec

JULY 1990

NASA

NASA Technical Memorandum 4200

Static Wind-Tunnel and Radio-Controlled Flight Test Investigation of a Remotely Piloted Vehicle Having a Delta Wing Planform

Long P. Yip, David J. Fratello,
and David B. Robelen
Langley Research Center
Hampton, Virginia

George M. Makowiec
Vigyan Research Associates, Inc.
Hampton, Virginia

NASA
National Aeronautics and
Space Administration
Office of Management
Scientific and Technical
Information Division

1990

Abstract

At the request of the U.S. Marine Corps, an exploratory wind-tunnel and flight test investigation was conducted by the Flight Dynamics Branch at the NASA Langley Research Center to improve the stability, controllability, and general flight characteristics of the Marine Corps Exdrone RPV (remotely piloted vehicle) configuration. Static wind-tunnel tests were conducted in the Langley 12-Foot Low-Speed Tunnel to identify and improve the stability and control characteristics of the vehicle. The wind-tunnel test resulted in several configuration modifications, which included increasing the size of the elevator, rudder, and vertical tail; increasing the vertical tail moment arm; adding vertical wingtip fins; and adding leading-edge droops on the outboard wing panel to improve stall departure resistance. Flight tests of the modified configuration were conducted at the NASA Langley Plumtree Test Site to provide a qualitative evaluation of the flight characteristics of the modified configuration.

Introduction

In recent years, there has been keen interest in the military to develop remotely piloted, unmanned flight vehicles. The Exdrone RPV (expendable drone, remotely piloted vehicle) configuration is a low-cost unmanned flight vehicle being developed by the U.S. Marine Corps to provide support capabilities in various mission roles. The Exdrone RPV is basically a delta-wing configuration powered by a tractor propeller propulsion system. The vehicle has a relatively simple flight control system that uses a rate gyro to augment roll damping during flight. In preliminary flight tests conducted by the Marine Corps, the vehicle exhibited weak stability and control characteristics in low-speed flight, and a tendency to depart lateral-directionally near the stall. At the request of the Marine Corps, an exploratory wind-tunnel and flight test investigation was conducted by the Flight Dynamics Branch at the NASA Langley Research Center to improve the stability and control and general flight characteristics of the Exdrone RPV configuration.

In order to accomplish this objective, exploratory wind-tunnel and flight tests were conducted to determine the basic aerodynamic characteristics of the configuration, to identify problem areas, and to provide modifications for aerodynamic improvements. An initial wind-tunnel investigation was conducted in the Langley 12-Foot Low-Speed Tunnel on the baseline Exdrone RPV configuration as it was received from the Marine Corps. After completion of the wind-tunnel study, recommendations were made to the Marine Corps for several modification improvements. The modifications included increasing the size of the elevator, vertical tail, rudder, and aileron, and increasing the vertical tail moment arm. The ailerons were deflected differentially with greater up travel than down travel in order to minimize adverse yaw characteristics. Vertical wingtip fins were added to improve directional stability, and a leading-edge droop was added to the outboard wing panel to improve departure resistance. As a result of this study, the Marine Corps incorporated the modifications into a revised Exdrone RPV. Flight tests were conducted at the NASA Langley Plumtree Test Site to provide a qualitative evaluation of the flight characteristics of the modified configuration. The results of the wind-tunnel and flight tests are reported herein.

Symbols

All longitudinal forces and moments are referred to the stability axis system, and all lateral-directional forces and moments are referred to the body axis system.

b	wingspan, ft
C_L	lift coefficient, $\frac{\text{Lift}}{qS}$
C_l	rolling-moment coefficient, $\frac{\text{Rolling moment}}{qSb}$
ΔC_l	incremental rolling-moment coefficient
C_{l_β}	rolling-moment coefficient due to sideslip (positive stability indicated by negative values), per degree
C_m	pitching-moment coefficient, $\frac{\text{Pitching moment}}{qSc_{\text{ref}}}$
C_n	yawing-moment coefficient, $\frac{\text{Yawing moment}}{qSb}$
ΔC_n	incremental yawing-moment coefficient
C_{n_β}	yawing-moment coefficient due to sideslip, per degree
$C_{n_{\beta,\text{dyn}}}$	yaw divergence parameter, $C_{n_\beta} \cos\alpha - \frac{I_Z}{I_X} C_{l_\beta} \sin\alpha$
C_T	thrust coefficient, T/qS
C_Y	side-force coefficient, $\frac{\text{Side force}}{qS}$
ΔC_Y	incremental side-force coefficient
C_{Y_β}	side-force coefficient due to sideslip, per degree

c_{ref}	reference wing chord (theoretical root chord used), 4.458 ft
I_X, I_Z	mass moment of inertia about X- and Z-axis, respectively, slug-ft^2
q	free-stream dynamic pressure, psf
S	reference wing area, 21.24 ft^2
T	effective thrust, $\text{Drag}_{\text{propeller removed}} - \text{Drag}_{\text{propeller operating}}$
x	distance along chord line from leading edge to trailing edge, in. (see fig. 4(b))
y	distance from chord line to upper or lower surface, in. (see fig. 4(b))
α	angle of attack, deg
β	angle of sideslip, deg
δ_a	aileron deflection per side, positive trailing edge down, deg
δ_e	elevator deflection, positive trailing edge down, deg
δ_r	rudder deflection, positive trailing edge left, deg

Subscripts:

l	left
r	right

Abbreviations:

c.g.	center of gravity
L.E.	leading edge
RPV	remotely piloted vehicle
USMC	United States Marine Corps

Model and Tests

Two configurations of the USMC Exdrone RPV were tested in the Langley 12-Foot Low-Speed Tunnel. The first configuration tested was the baseline configuration furnished to NASA by the USMC. Figure 1 shows the baseline Exdrone configuration installed in the Langley 12-ft tunnel. A three-view sketch of the baseline configuration is shown in figure 2. The second configuration, also furnished by the USMC, was an Exdrone RPV modified according to recommendations from the initial wind-tunnel test of the baseline configuration in the Langley 12-ft tunnel. The modified Exdrone RPV is shown installed in the tunnel in figure 3. A three-view sketch of the modified Exdrone RPV configuration is presented in figure 4(a), which illustrates the major modifications made to the baseline Exdrone RPV. The modifications included increasing the size of the elevator, vertical tail, rudder, and aileron; and increasing the vertical tail moment arm. The aileron deflection schedule was modified to provide unequal, differential motion with more up deflection than down in order to minimize adverse yaw characteristics. Vertical wingtip fins were added to improve directional stability, and a leading-edge droop was added to the outboard wing panel to improve stall departure resistance. The leading-edge droop modification was applied to the wingtip extension from the wingtip fin juncture to the tip (see fig. 4(b)). The wingtip fin was recessed 0.625 in. to provide for a small notch (see fig. 4). The intention of having a notch was to enhance the vortex flow from the snag inboard edge of the leading-edge droop to keep the flow attached on the wingtip panel at high angles of attack (see ref. 1). By keeping the flow attached on the wingtip panel, roll damping of the configuration is increased (see refs. 2 to 5).

Wind-Tunnel Tests

The static wind-tunnel tests were conducted in the Langley 12-Foot Low-Speed Tunnel. This wind tunnel is used primarily as a diagnostic facility for exploratory research in the area of stability and control on various configurations. The test section of the wind tunnel has a 12-ft octagonal cross section and is 15 ft in length. Tests were conducted at a nominal free-stream dynamic pressure of 4 psf, which corresponds to a velocity of approximately 58 ft/sec and to a Reynolds number of approximately 1.67 million based on the reference chord. This tunnel condition approximated full-scale flight conditions near the stall. The angle-of-attack range of the tests was from 0° to 30°, and the angle-of-sideslip range was from −16° to 16°. Although the model size relative to the tunnel size was large, no corrections were made to account for tunnel blockage or for the jet boundary. Linear correction methods were not applied because they were not applicable in the area of high-angle-of-attack aerodynamics. For the wind-tunnel tests, the fuselage was structurally modified to accommodate a six-component strain-gage balance for measuring aerodynamic forces and moments. Power-on tests were conducted using an air turbine motor to supply power to the propeller. A commercially available propeller having a 20-in. diameter and a 14-in. pitch was used for this part of the test. The propeller was the same type as that used for the flight tests. Values of C_T from 0 to 0.75 were obtained in the wind

tunnel by lowering the free-stream dynamic pressure. For the condition of $C_T = 0$, the propeller was not installed on the model. The reference moment center was 28.75 in. from the fuselage trailing edge for the baseline configuration. In the modified model, the reference moment center was moved aft to 27.67 in. from the trailing edge of the fuselage section.

Radio-Controlled Flight Tests

Qualitative flight test evaluations were performed at the NASA Langley Plumtree Test Site on the modified configuration to confirm the effect of modification improvements on stability, controllability, and general flight behavior. Photographs of the modified Exdrone at the test site are shown in figure 5. A description of the test site is found in reference 6. The Exdrone RPV was equipped with a radio-controlled flight system that included an onboard receiver, control servos, and batteries for electrical power. A commercially available flight control system having eight channels of control inputs was used to pilot the vehicle. A schematic of the control system is shown in figure 6. The command control transmitter allowed the rudder inputs to be integrated with the aileron inputs. A rudder-to-aileron interconnect could be switched on to provide the vehicle with reduced bank angles in turning flight. A rate gyro was used to augment the roll damping of the configuration.

Power for the vehicle was provided by a modified, two-stroke chain saw engine that developed about 6.6 hp from a 5.8-in^3 displacement. The propeller had a 20-in. diameter and a 14-in. pitch and was located in a tractor position on the RPV. The vehicle weighed 35 lb empty and was designed to carry 26 lb of payload with 4 lb of fuel for a nominal maximum takeoff gross weight of 65 lb. Flight characteristics were initially obtained on a lightly loaded configuration of 45 lb gross weight at takeoff. The weight of the vehicle was eventually increased beyond the nominal maximum takeoff gross weight of 65 lb to 70.5 lb during the flight test. The vehicle weight was not further increased because of the limitations of a relatively short runway length (approximately 250 ft) for landing operations.

The vehicle was launched on a takeoff dolly by stretching bungee chords a distance of approximately 80 to 90 ft to assist in acceleration of the vehicle during takeoff as shown in figure 7. For recovery of the vehicle, a front skid pad and rear skid wires were attached to the underside of the vehicle to aid in the touchdown and braking of the vehicle during the landing ground run.

The basic flight test setup is illustrated in figure 8. The vehicle was flown by remote control by either an outdoor visual pilot or an indoor video pilot. An onboard video camera was used to transmit real-time display of the forward view from the vehicle to the ground-based video pilot. The onboard camera display was also helpful in providing additional information for evaluation purposes. An externally mounted tracking camera, which is part of the facility at the Langley Plumtree Test Site, was used to follow the motions of each flight maneuver. The flights were recorded on videocassettes for both the onboard camera and the ground-based tracking camera.

The flight characteristics of the configuration were evaluated using the following flight maneuvers:

High-angle-of-attack maneuver. The vehicle was flown with wings level and power reduced to idle at the start of the maneuver. The control stick was gradually pulled to a full-back position and held at that position with inputs of aileron and rudder to maintain heading. After the vehicle was stabilized at full-back stick, the throttle was then gradually increased until full power was applied to determine the effects of power at high-angle-of-attack flight conditions.

Doublet maneuvers. With the vehicle trimmed in level flight, rapid elevator or rudder inputs were used to excite the configuration for either longitudinal or lateral-directional motions. For each evaluation, the control surface was deflected from full negative to full positive values to perturb the motions of the vehicle about a particular axis. The control stick was then quickly released to the previously determined trimmed settings, and the damping characteristics of the vehicle were evaluated by observing its motions following the doublet inputs.

Several modification improvements resulted from the flight tests. Initial flights were conducted with nominal control settings of ailerons deflected symmetrically from $-17°$ to $+17°$ and the rudder deflected from $-15°$ to $+15°$. Since lateral-directional control power was perceived to be weak at the higher angles of attack, aileron and rudder controls were increased. The aileron control power was increased by extending the aileron chord and by increasing the travel for aileron deflection. In addition, the aileron control surfaces were deflected differentially with a travel of 7° trailing-edge down and 23° trailing edge up to minimize adverse yaw effects. Rudder control settings were increased to $\pm 25°$. The tip fin area was increased by approximately 25 percent to increase directional stability, which was perceived to be weak at high angles of attack. Engine thrust was offset 2.5° nose right to reduce out of trim yawing moments due to power effects. In order to provide additional pitch trim to offset the required elevator trim setting, the

left and right aileron control surfaces were preset to 4° trailing edge up.

Results and Discussion

Wind-Tunnel Test

Longitudinal aerodynamic characteristics. Figure 9 shows the lift and pitching-moment characteristics of the baseline configuration with elevator deflections of 0°, 10°, and 20° trailing edge up. The data indicate linear lift and pitching-moment curves for angle-of-attack values up to about 12°. Above 12° angle of attack, the configuration exhibited nonlinear aerodynamic characteristics that were probably caused by the development of spanwise flow associated with a swept wing planform. The baseline configuration was longitudinally stable throughout the test angle-of-attack range. For the baseline configuration at its nominal center-of-gravity location, the longitudinal static margin was about 6 percent, based on the reference chord. The maximum nose-up pitch control for the baseline configuration (20° trailing-edge up elevator deflection) provided a maximum achievable trimmed angle of attack of about 7°, which corresponds to a maximum trimmed lift coefficient of about $C_L = 0.25$. For this designed c.g. location, the relatively low value of maximum trimmed lift achieved on the baseline Exdrone RPV configuration limited the approach speed and payload-handling capabilities of the vehicle.

In order to increase the pitch trim capability of the vehicle, several configuration changes were considered. These changes included relaxing the longitudinal stability, increasing the elevator deflection, and increasing the elevator size. Because the vehicle was constrained to a limited c.g. envelope from payload considerations and because of the need to keep the control system simple, relaxing the longitudinal static stability with large changes in the c.g. location was not acceptable as a means for achieving higher trim angle of attack. Also, deflecting the elevator to a higher setting would have caused flow separation and put the elevator control surface in a nonlinear angle range. Therefore, a chord extension to the elevator control surface was used to increase the amount of pitch control for nose-up trim.

The modified Exdrone RPV configuration incorporated the larger elevator chord and was wind-tunnel tested with the moment reference center at 2.5 percent of the reference chord aft of the baseline configuration. In addition, the ailerons were rigged symmetrically 4° trailing edge up to provide additional nose-up moments for pitch trim. With these configuration changes, the longitudinal aerodynamic characteristics of the modified Exdrone RPV configuration at various elevator deflections are shown in figure 10. The data indicate stable pitching-moment characteristics for the test angle-of-attack range. Maximum trimmed angle of attack for the modified configuration was about 15°, which corresponds to a trimmed lift coefficient of about 0.7. These trimmed values are significantly larger than those for the baseline configuration. In terms of minimum level-flight speeds, the increased lift capability for a nominal vehicle gross weight of 65 lb reduced the minimum flight speed from 69 mph for the baseline configuration to 41 mph for the modified configuration.

The effect of leading-edge droop modification on the longitudinal aerodynamic characteristics is shown on figure 11. The data indicate that the leading-edge droop produced a flatter lift curve at the stall. From previous research on leading-edge droop modifications to the outboard panel of light general aviation airplanes, significant improvements can be obtained in the post-stall lift characteristics of the outer portion of the wing (for example, see ref. 2). Although the effect of the leading-edge droop on the overall lift characteristics of the Exdrone RPV was small, its effect on the outboard portion of the wing was apparently significant, as indicated by the improved stall departure characteristics from flight tests.

The effect of power on the longitudinal aerodynamic characteristics of the modified Exdrone RPV is shown in figure 12. The thrust coefficients tested represent power conditions for the RPV up to maximum thrust at stall conditions. As expected, power effects increased the lift curve slope and the maximum lift of the configuration. In addition, power effects decreased the longitudinal stability in the low to moderate angle-of-attack range. This decrease in longitudinal stability was apparently caused by the propeller normal force and the propeller slipstream interaction with the wing.

The effect of power on longitudinal trim is shown in figure 13 for the modified Exdrone configuration with the elevator set at the maximum deflection of 18° trailing edge up. A comparison of figures 12 and 13 indicates that the slipstream of the propeller increased the dynamic pressure over the elevator control surface, which resulted in increased pitch control authority. From the power-off condition to the maximum thrust setting tested, the maximum trimmed angle of attack increased from about 14° to about 21°, and the maximum trimmed lift coefficient increased from about 0.6 to 1.25.

Lateral-directional characteristics. Figure 14 shows the lateral-directional stability characteristics of the baseline configuration in the form of the stability derivatives C_{Y_β}, C_{n_β}, and C_{l_β}. The data show that the baseline configuration exhibited stable dihedral effect, but low values of directional stability. The data also show that a vertical canard (see fig. 2), which was placed on the baseline configuration to increase directional control, significantly weakened the directional stability of the baseline configuration. The value of C_{n_β} approached zero at an angle of attack of about 12°.

Several changes were incorporated into the modified configuration to improve its directional stability (see fig. 4). These modifications included increasing the rudder area, adding ventral tail area, moving the vertical tail 6 in. aft, and adding wingtip fins. The lateral-directional stability characteristics of the baseline and modified Exdrone configurations are compared in figure 15. The data indicate that the modifications more than doubled the directional stability C_{n_β} of the baseline configuration without significantly affecting the dihedral effect $-C_{l_\beta}$ in the normal operating angle-of-attack range.

The contribution of various configuration components on the lateral-directional stability characteristics of the modified configuration is shown by the data in figure 16. The data show the incremental effects due to the leading-edge droop modification, the addition of wingtip fins, and the addition of vertical tail area. The configuration without the vertical tail was neutrally stable in yaw and became unstable near the stall onset ($\alpha = 12°$ to 16°). The addition of the vertical tail provided directional stability through the stall angle of attack; however, the directional stability became unstable above $\alpha = 24°$. This yaw instability was probably caused by large vortical flow at high angles of attack, which at sideslip causes a sidewash contribution on the flow at the vertical tail area (see ref. 7). The addition of the wingtip fins provided a significant increment of directional stability at low to moderate angles of attack. Since the tip fin area was added mostly to the lower surface, the effective dihedral was not increased. At angles of attack above 20°, the configuration exhibited unstable values of C_{l_β}. The addition of the wingtip fin and the leading-edge droop reduced this level of instability at the higher angles of attack.

The effects of power on the lateral-directional stability characteristics of the modified Exdrone configuration are shown by the data of figure 17. Without power, the configuration exhibited unstable dihedral effect at test angles of attack of $\alpha = 20°$ to 24° and unstable directional stability at test angles of attack of $\alpha = 22°$ to 26°. With power on, the configuration exhibited stable lateral-directional stability throughout the test angle-of-attack range and a significant increase in lateral-directional stability at the higher test angles of attack. The increase in the stability of the configuration due to power effects at high angles of attack was probably caused by the improvements in dynamic pressure and sidewash from the interaction of the propeller slipstream and the vertical tail. At the maximum thrust setting ($C_T = 0.75$), the configuration exhibited stable but decreased values of directional stability at low to moderate angles of attack. This decrease in directional stability at the high-power setting is likely associated with the amount of side force generated by the tractor propeller in sideslip conditions, which apparently offsets the increase in directional stability due to the improved flow on the vertical tail.

Lateral-directional control characteristics of the baseline configuration for $C_T = 0$ are shown in figures 18 and 19 for aileron and rudder control deflections, respectively. The aileron controls of the baseline configuration were set up for equal but opposite deflections on the left and right sides. Aileron control power of the baseline configuration is shown in the data in figure 18 for several deflection settings for only the left aileron control surface. The data indicate that the aileron control effectiveness was nonlinear with increasing aileron deflection. The configuration with ailerons set at $\delta_{a,l}/\delta_{a,r} = -30°/0°$ showed about as much incremental rolling moment ΔC_l as the configuration with $\delta_{a,l}/\delta_{a,r} = -20°/0°$. Aileron control power remained relatively constant throughout the test angle-of-attack range. The data of figure 19 indicate that the rudder control authority of the configuration was relatively constant throughout the angle-of-attack range.

Lateral-directional control characteristics of the modified configuration at $C_T = 0$ are shown in figures 20 and 21 for aileron and rudder control deflections, respectively. For a maximum total differential aileron deflection of 30°, a comparison of figures 18 and 20 indicates that the modified configuration exhibited an increase of maximum roll control over the baseline configuration. In addition, the aileron controls of the modified configuration with their offset in up travel provided more favorable yaw characteristics. The effect of the rudder on the modified configuration is shown by the data of figure 21. Since the directional stability of the modified configuration was significantly increased, modifications were made to increase rudder control power to compensate for flight conditions in sideslip. The increase in rudder control power was accomplished by adding rudder size and moment arm. The data show that these

modifications provided about 50 percent more rudder control authority than that of the baseline configuration. The data also show that the rudder control authority was not significantly reduced at angles of attack up to 22°.

The effect of power on the rudder control authority is shown by the data of figure 22. The data indicate that the effects of power are quite large on the rudder control authority of this configuration. At low angles of attack, the yawing moment due to power with the maximum rudder deflection was about 4 times that of the power-off configuration. At angles of attack above 20°, there was a reduction in the yaw control authority; however, yaw control was still significantly greater with power on than with power off.

A plot of the yaw divergence parameter $C_{n_{\beta,\mathrm{dyn}}}$ for the configuration with the leading-edge droop off and on is presented in figure 23. The data are generally in good agreement with the flight test results and show that, with power on, the leading-edge droop had very stable values of $C_{n_{\beta,\mathrm{dyn}}}$ at high angles of attack. No static tests were made with power on for the configuration with the leading-edge droop off.

Flight Test Results of the Modified RPV

Qualitative flight test evaluations were conducted on the modified Exdrone RPV configuration, described in the "Model and Tests" section of this report. Since the baseline configuration was unavailable for flight test evaluation, only the modified Exdrone RPV was tested in flight. Flight tests of the modified Exdrone configuration were initially conducted on a lightly loaded configuration of 45 lb gross weight at takeoff. During the test, the weight of the vehicle was eventually increased beyond the designed maximum takeoff gross weight of 65 to 70.5 lb. Flight test maneuvers included the high-angle-of-attack and doublet flight maneuvers described earlier in the flight test description section. The high-angle-of-attack maneuvers were assessed with the leading-edge droop on and off.

Longitudinal flight characteristics. The longitudinal stability and control characteristics of the modified Exdrone configuration were generally rated as very satisfactory by the test pilots over the nominal operating range of flight conditions tested. The modified vehicle exhibited stable short-period damping characteristics about the pitch axis, with the pitch motions completely damped within one cycle of oscillation. At higher wing loadings, the configuration was less responsive to controls but was steadier in flight because of its higher wing loading, which made the vehicle less sensitive to wind gusts. During the evaluation, the vehicle with the leading-edge droop off was controllable with full-back stick and with the throttle set to idle power. With the application of power, the vehicle could be trimmed to a higher angle of attack and had more control power in pitch. However, with full power inputs, the maximum achievable angle of attack on the configuration with the leading-edge droop off was limited by a lateral-directional stall departure despite corrective controls. With the leading-edge droop on, no uncontrollable stall departures occurred on this configuration for all conditions tested, and therefore the leading-edge droop configuration could be flown to higher angles of attack than the configuration without the leading-edge droop at full-back stick and full power. In addition to providing the configuration with improved departure resistance, the leading-edge droop modification did not change the pitch trim flight characteristics in the normal operating range of flight.

Lateral-directional flight characteristics. The lateral-directional flight characteristics of the modified Exdrone RPV configuration were considered to be very good. In the low to moderate angle-of-attack range of flight, the modified Exdrone vehicle exhibited good lateral-directional stability characteristics, responded well to lateral-directional control inputs, and exhibited good damping characteristics in response to aileron/rudder inputs. The modified Exdrone vehicle was also flown with the small chord aileron control surfaces. With the small chord ailerons, the vehicle was considered to be slow in roll response; whereas, with the larger chord ailerons of the modified configuration, the vehicle was considered satisfactory in roll response. With the roll rate gyro turned on, the lateral responsiveness of the vehicle, as expected, was reduced, but overall lateral-directional flying qualities were greatly improved.

The lateral-directional flight characteristics of the modified configuration at high angles of attack were evaluated with the leading-edge droop on and off. At high angles of attack, with test conditions of full-back stick input and at idle power, the configuration without the leading-edge droop modification was marginally controllable in flight and required constant attention to roll and yaw control inputs to prevent a lateral-directional stall departure. With power on, the configuration with the leading-edge droop off exhibited a roll departure despite full corrective control. This departure characteristic was observed on the configuration with the roll rate gyro turned either on or off.

With the leading-edge droop installed, the lateral-directional flight characteristics of the vehicle were significantly improved at high angles of attack. This improvement was likely due to increased roll damping. Although dynamic force tests were not conducted to measure roll damping, flight tests in the power-on condition, which permitted trimmed flights to high angles of attack, indicated that the addition of the leading-edge droop greatly reduced the roll-off tendency that was observed on the configuration with the leading-edge droop off.

Summary of Results

At the request of the U.S. Marine Corps, an exploratory wind-tunnel and flight test investigation was conducted by the Flight Dynamics Branch at the NASA Langley Research Center to improve the stability, controllability, and general flight characteristics of the Marine Corps Exdrone RPV (remotely piloted vehicle) configuration. The investigation included exploratory wind-tunnel static tests in the Langley 12-Foot Low-Speed Tunnel and radio-controlled flight tests at the NASA Langley Plumtree Test Site.

The wind-tunnel static tests identified several deficiencies in the longitudinal and lateral-directional stability and control characteristics of the baseline configuration, which led to several modifications for improved stability and control characteristics. The configuration modifications that proved to be most effective included increasing the size of the elevator, vertical tail, rudder, and aileron; increasing the vertical tail moment arm; adding vertical wingtip fins; and adding leading-edge droops to the outboard wing panel.

The results of the radio-controlled flight tests showed that the modified configuration had good longitudinal and lateral-directional flight characteristics over the test angle-of-attack range. The configuration was very maneuverable and responsive to control inputs, exhibited good damping characteristics, and was easily flyable through the stall with no departure tendencies.

NASA Langley Research Center
Hampton, VA 23665-5225
May 9, 1990

References

1. Meyer, H. F.; Yip, L. P.; Perkins, J. N.; and Vess, R. J.: Experimental Investigation of the High Angle of Attack Characteristics of a High Performance General Aviation Aircraft. *A Collection of Technical Papers—AIAA 7th Applied Aerodynamics Conference*, July–Aug. 1989, pp. 733–742. (Available as AIAA-89-2237-CP.)
2. Staff of Langley Research Center: *Exploratory Study of the Effects of Wing-Leading-Edge Modifications on the Stall/Spin Behavior of a Light General Aviation Airplane.* NASA TP-1589, 1979.
3. Yip, Long P.; King, Patrick M.; Muchmore, C. Byram, and Davis, Pat: Exploratory Wind-Tunnel Investigation of the Stability and Control Characteristics of Advanced General Aviation Configurations. AIAA-86-2596, Sept.–Oct. 1986.
4. Yip, Long P.; Robelen, David B.; and Meyer, Holly F.: Radio-Controlled Model Flight Tests of a Spin Resistant Trainer Configuration. AIAA-88-2146, May 1988.
5. Johnson, Joseph L., Jr.; Yip, Long P.; and Jordan, Frank L., Jr.: Preliminary Aerodynamic Design Considerations for Advanced Laminar Flow Aircraft Configurations. *Laminar Flow Aircraft Certification*, Louis J. Williams, compiler, NASA CP-2413, 1986, pp. 185–225.
6. Fratello, David J.; Croom, Mark A.; Nguyen, Luat T.; and Domack, Christopher S.: Use of the Updated NASA Langley Radio-Controlled Drop-Model Technique for High-Alpha Studies of the X-29A Configuration. *A Collection of Technical Papers—AIAA Atmospheric Flight Mechanics Conference*, Aug. 1987, pp. 305–317. (Available as AIAA-87-2559.)
7. Chambers, Joseph R.; and Anglin, Ernie L.: *Analysis of Lateral-Directional Stability Characteristics of a Twin-Jet Fighter Airplane at High Angles of Attack.* NASA TN D-5361, 1969.

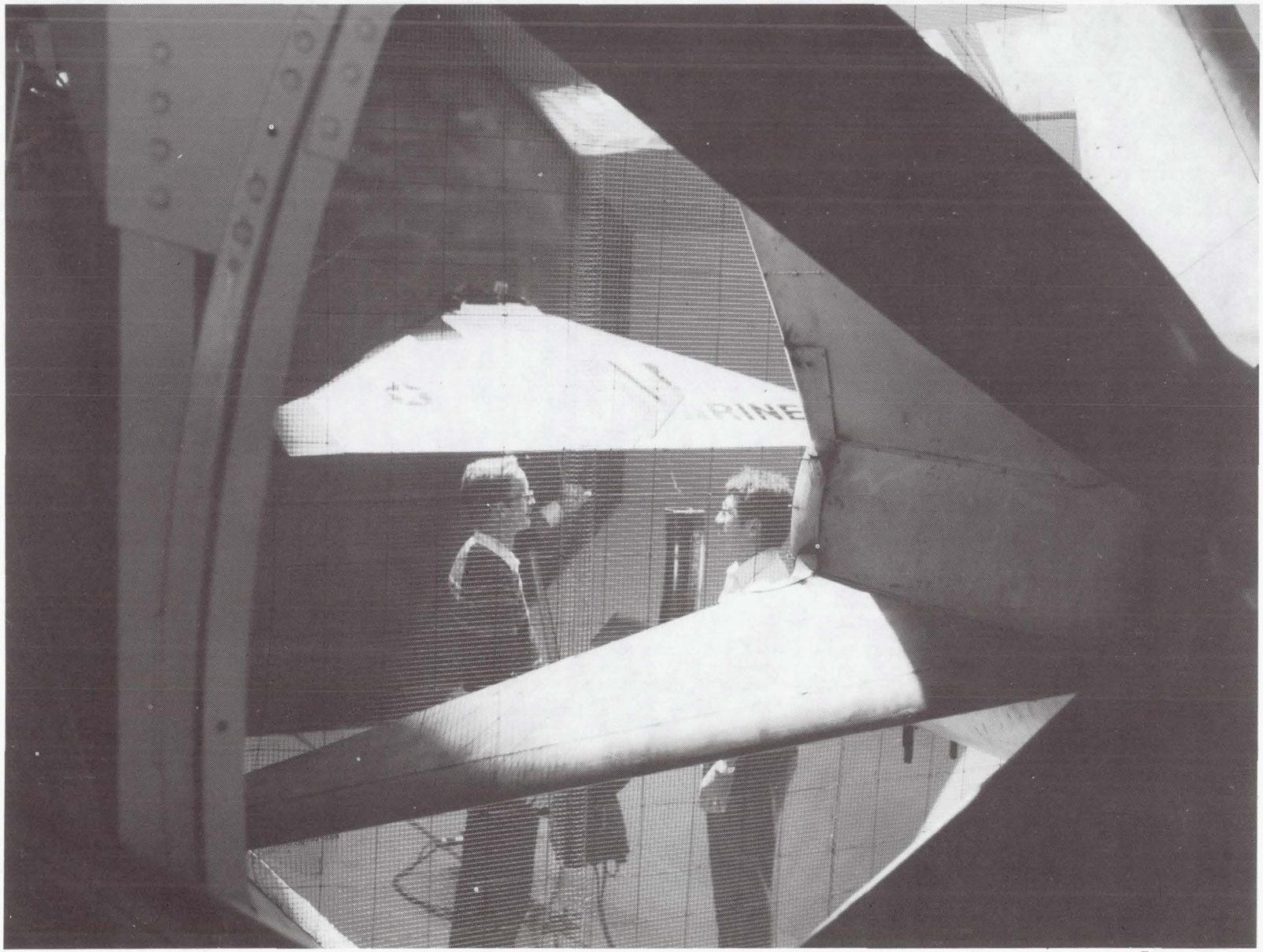

L-87-10,519

Figure 1. Baseline Exdrone RPV configuration installed in the Langley 12-Foot Low-Speed Tunnel.

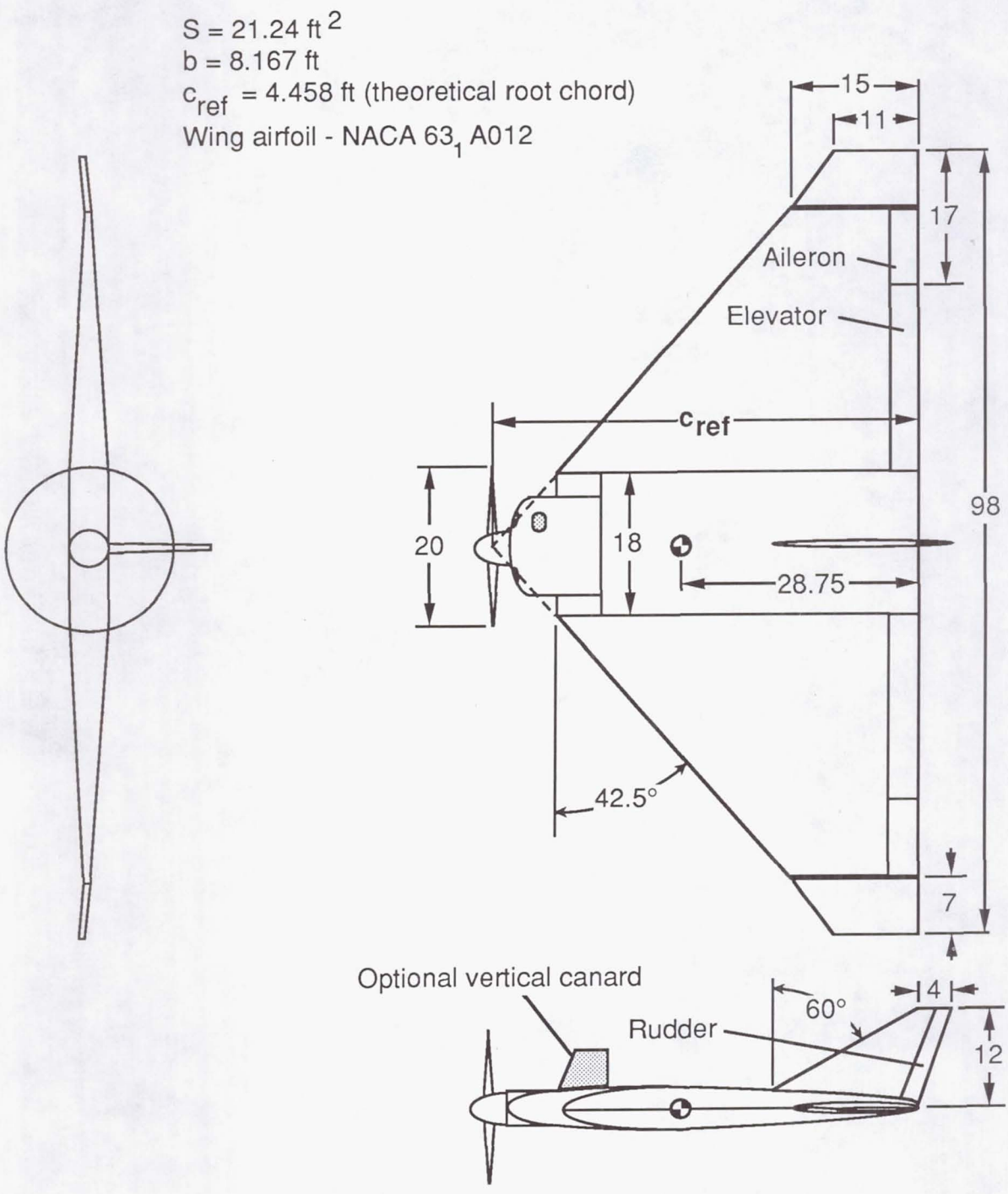

Figure 2. Three-view sketch of baseline Exdrone RPV configuration. Dimensions are in inches unless otherwise specified.

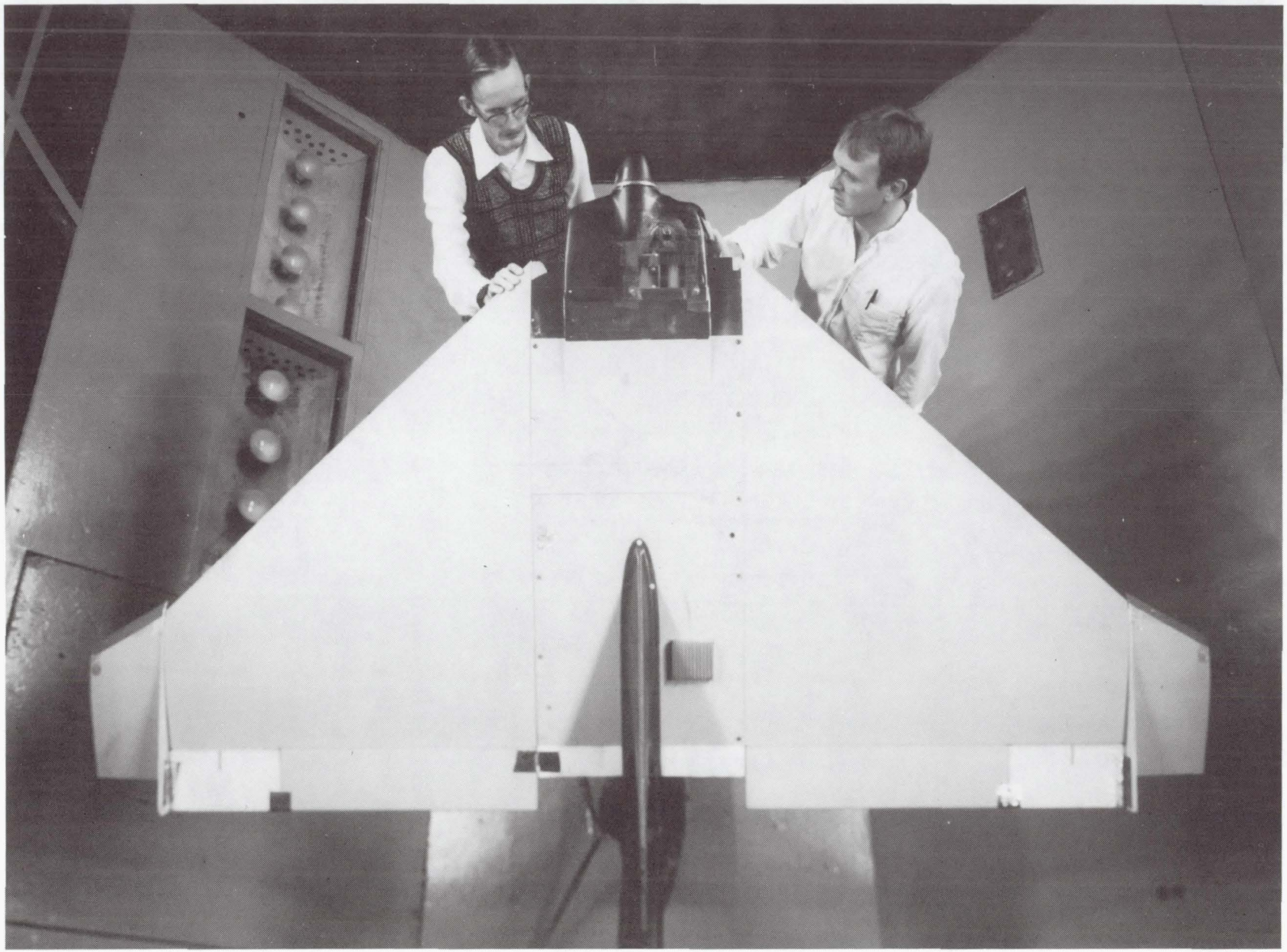

L-88-11,707

Figure 3. Modified Exdrone RPV installed in the Langley 12-Foot Low-Speed Tunnel.

$S = 21.24\ ft^2$
$b = 8.167$ ft
$c_{ref} = 4.458$ ft (theoretical root chord)

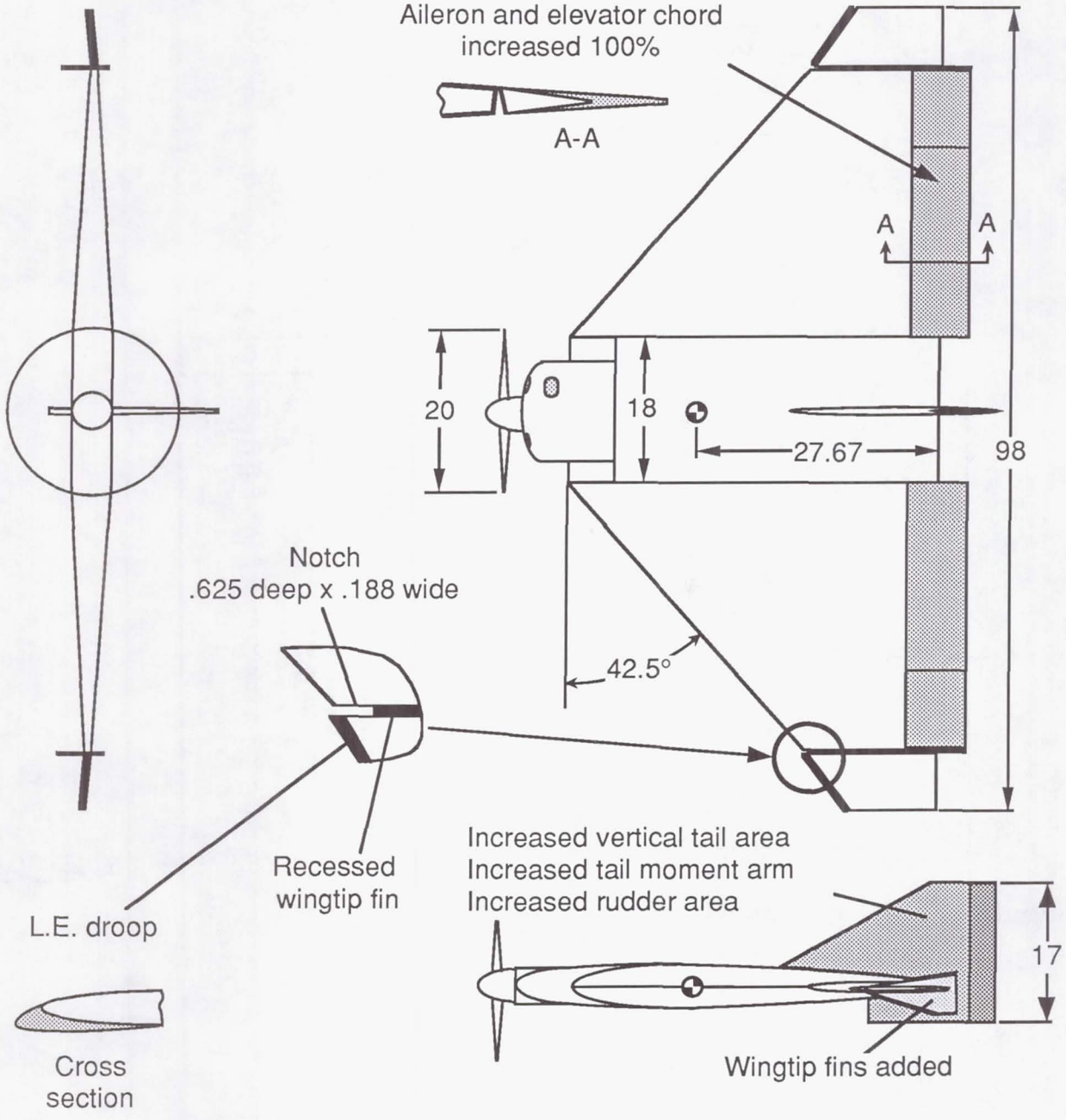

(a) Overview.

Figure 4. Three-view sketch of modified Exdrone RPV configuration. Dimensions are in inches unless otherwise specified.

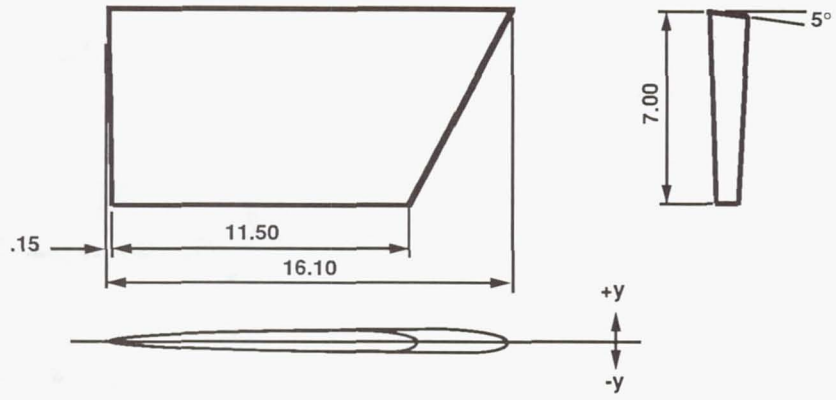

Airfoil coordinates

Root chord			Tip chord		
x_{root}	y_{upper}	y_{lower}	x_{tip}	y_{upper}	y_{lower}
-0.65	-0.54	-0.54	-0.50	-0.40	-0.40
-0.60	-0.35	-0.68	-0.40	-0.15	-0.55
-0.50	-0.20	-0.76	-0.30	-0.05	-0.59
-0.40	-0.10	-0.79	-0.20	0.05	-0.59
-0.30	0.02	-0.81	-0.10	0.11	-0.59
-0.20	0.09	-0.81	0.00	0.18	-0.59
-0.10	0.16	-0.82	0.20	0.27	-0.59
0.00	0.22	-0.82	0.50	0.41	-0.59
0.20	0.34	-0.82	1.00	0.50	-0.60
0.40	0.40	-0.83	1.50	0.56	-0.60
0.70	0.49	-0.83	2.00	0.60	-0.60
1.00	0.57	-0.83	2.50	0.62	-0.62
1.50	0.66	-0.83	3.00	0.65	-0.65
2.00	0.74	-0.82	4.00	0.68	-0.68
2.50	0.79	-0.82	5.00	0.66	-0.66
3.00	0.84	-0.84	6.00	0.63	-0.63
3.50	0.87	-0.87	7.00	0.56	-0.56
4.00	0.89	-0.89	8.00	0.43	-0.43
5.00	0.91	-0.91	9.00	0.31	-0.31
6.00	0.91	-0.91	10.00	0.19	-0.19
7.00	0.89	-0.89	11.00	0.07	-0.07
8.00	0.85	-0.85			
9.00	0.79	-0.79			
10.00	0.70	-0.70			
11.00	0.59	-0.59			
12.00	0.47	-0.47			
13.00	0.35	-0.35			
14.00	0.23	-0.23			
15.00	0.12	-0.12			
15.45	0.07	-0.07			

(b) Wingtip geometry.

Figure 4. Concluded.

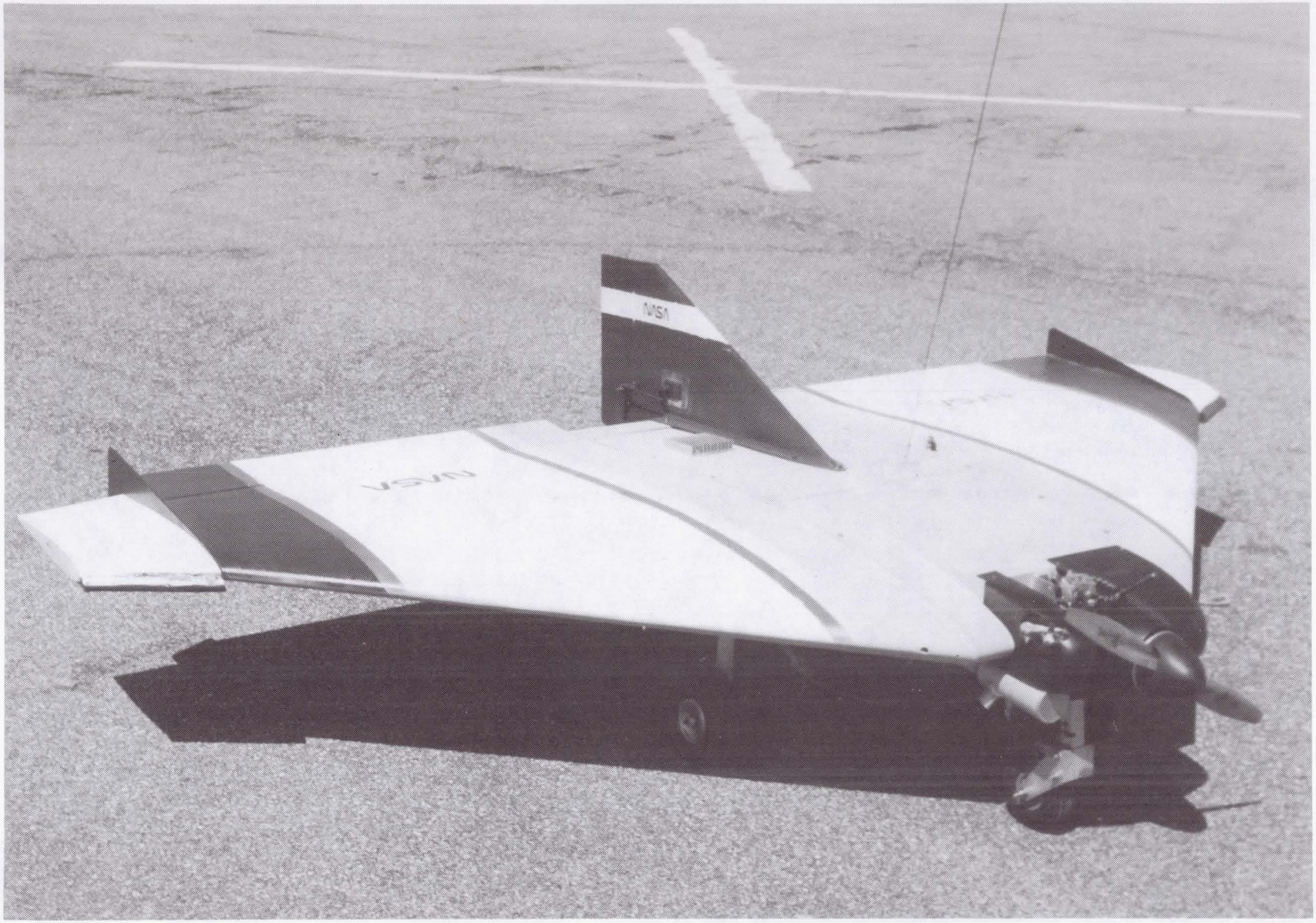

L-88-9679

(a) Three-quarter front view.

Figure 5. Modified Exdrone configuration at the Langley Plumtree Test Site.

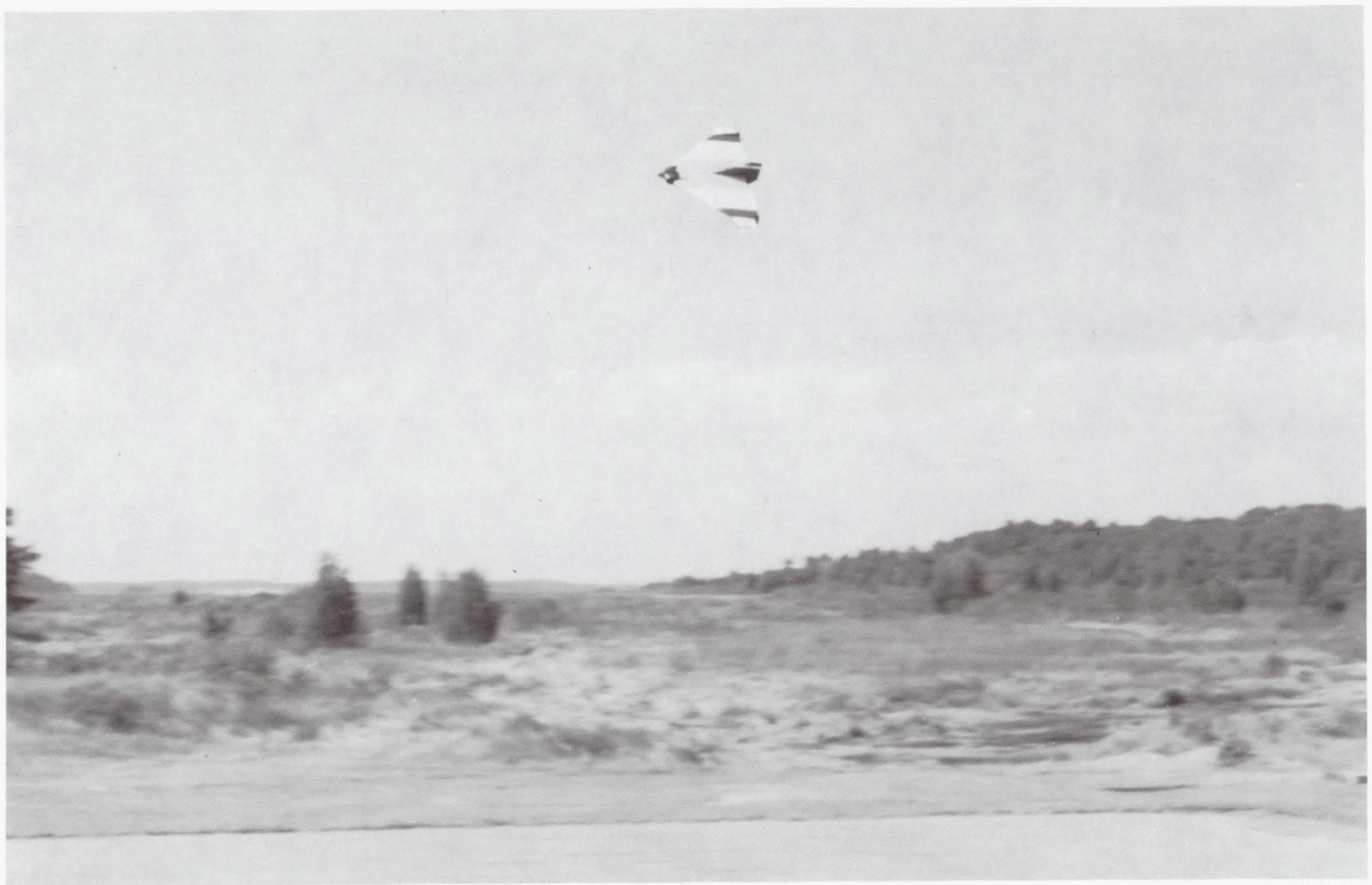

L-88-9693

(b) Modified configuration in flight.

Figure 5. Continued.

L-88-9694

(c) During landing approach.

Figure 5. Concluded.

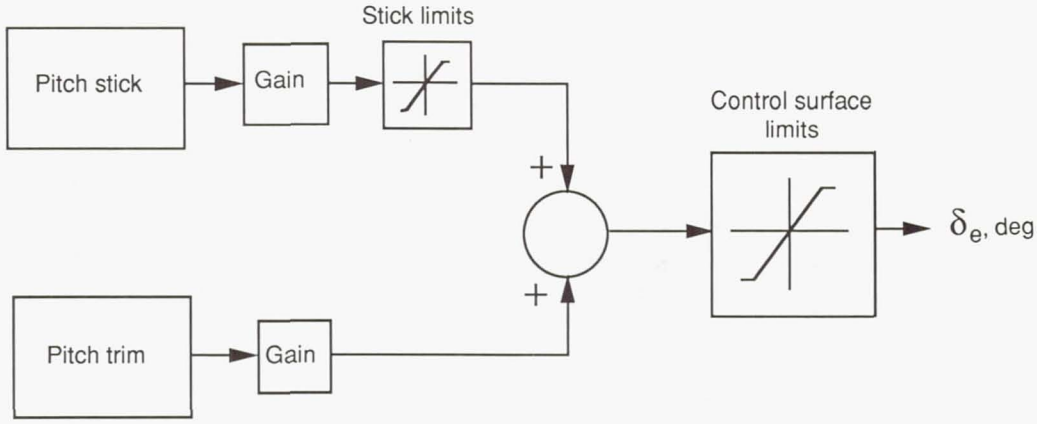

(a) Pitch.

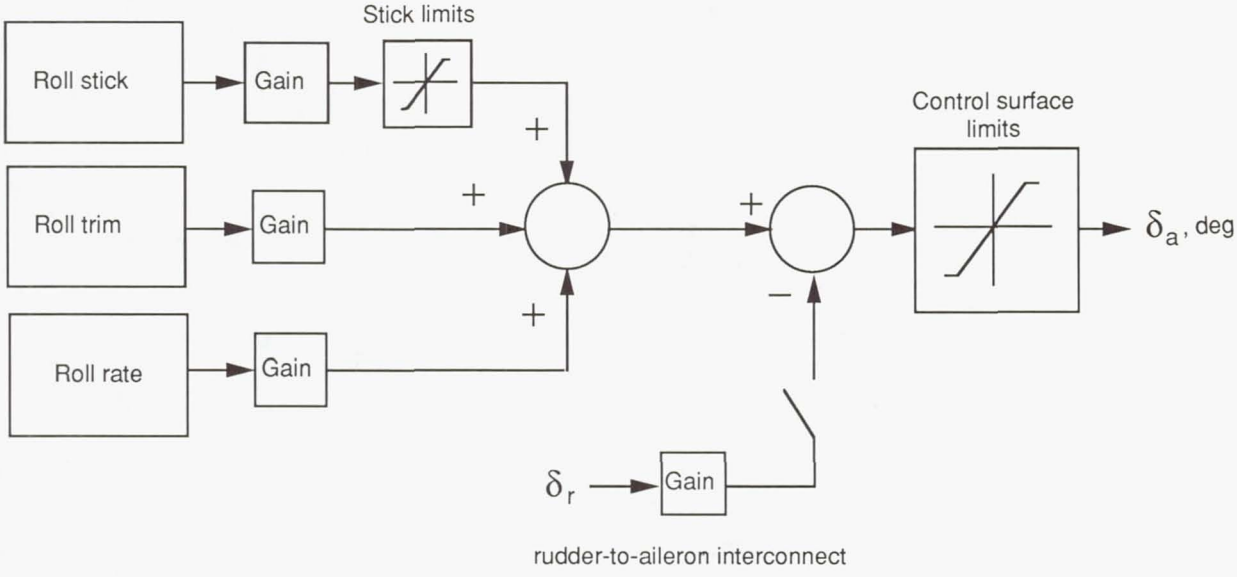

(b) Roll.

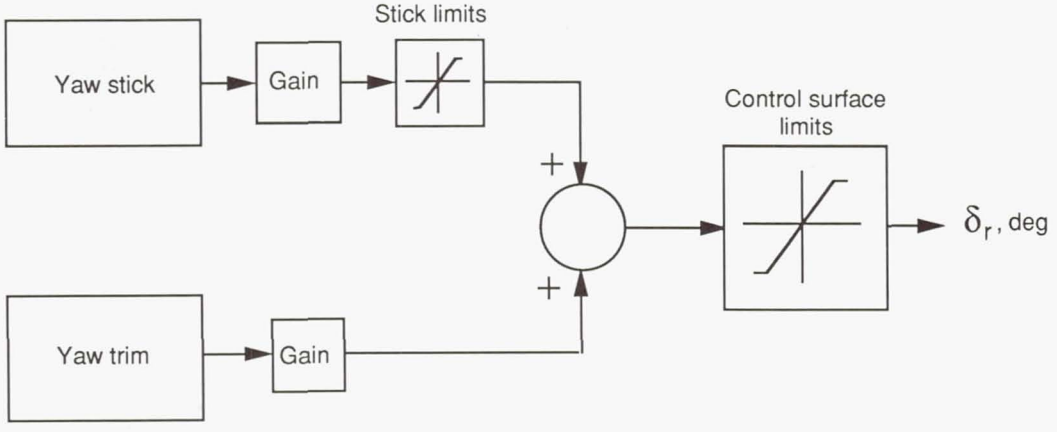

(c) Yaw.

Figure 6. Schematic of control system.

L-88-9686

Figure 7. Launch setup at the Langley Plumtree Test Site for the Exdrone RPV.

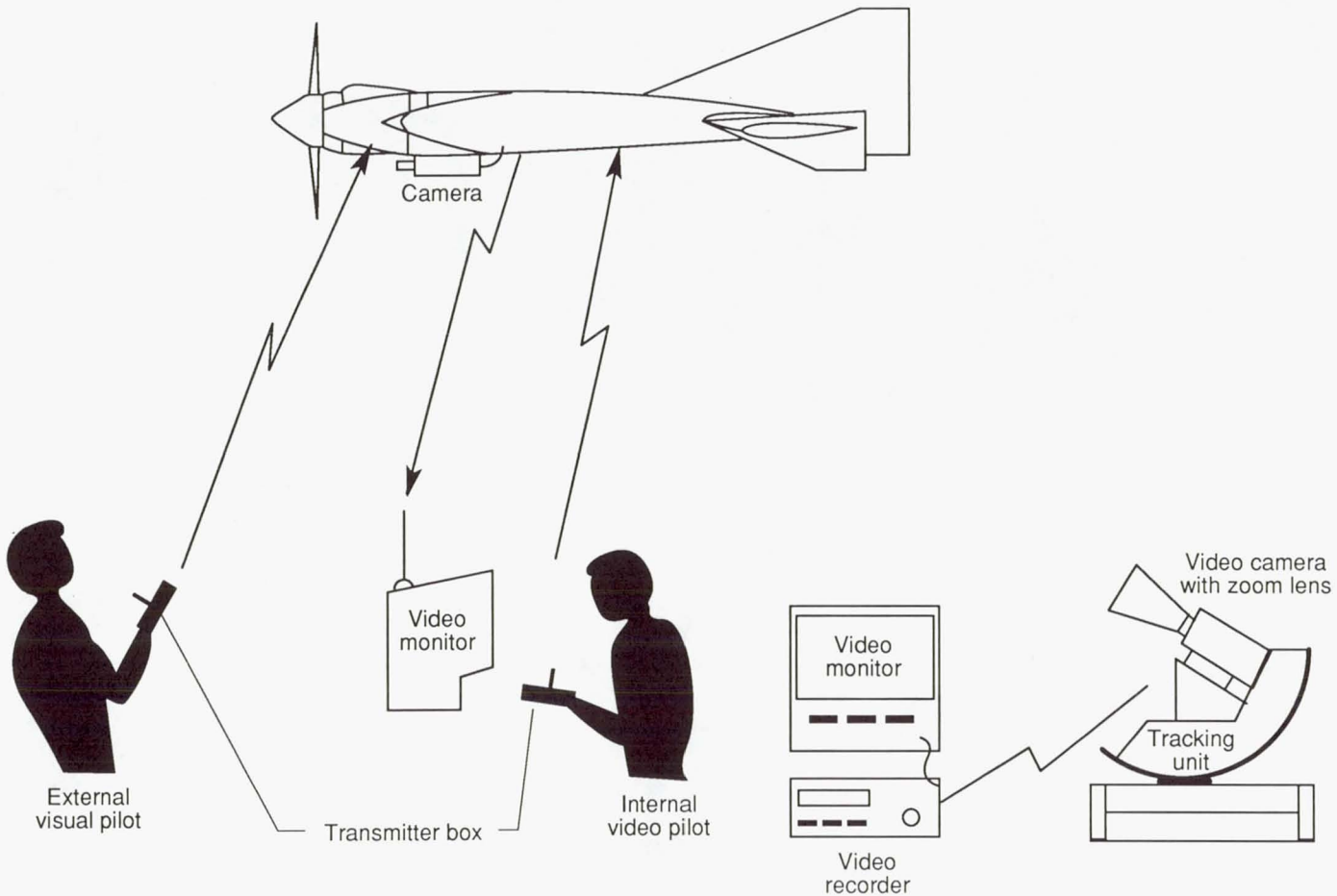

Figure 8. Illustration of flight test setup.

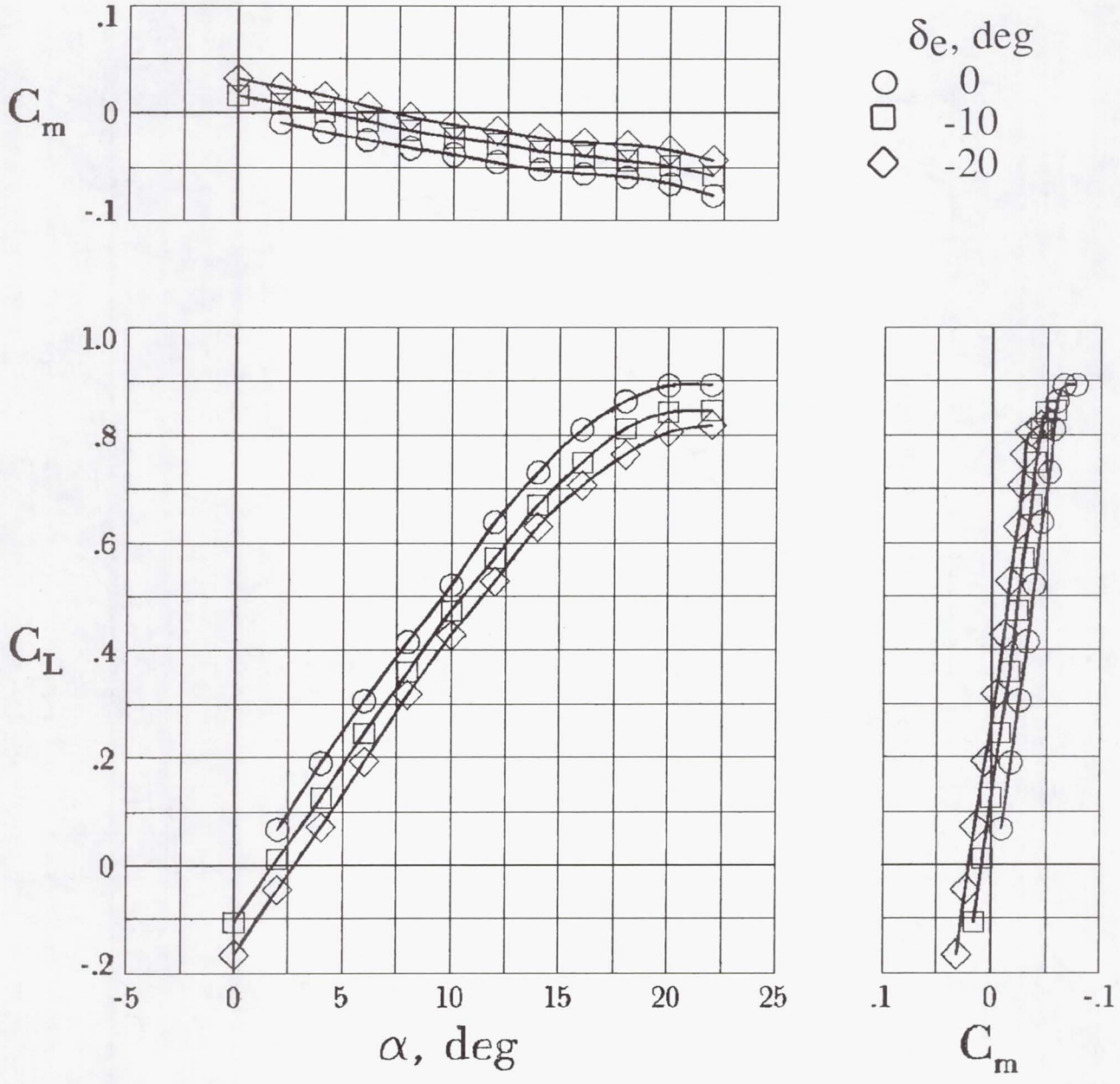

Figure 9. Effect of elevator deflection on the longitudinal aerodynamic characteristics of the baseline Exdrone RPV configuration.

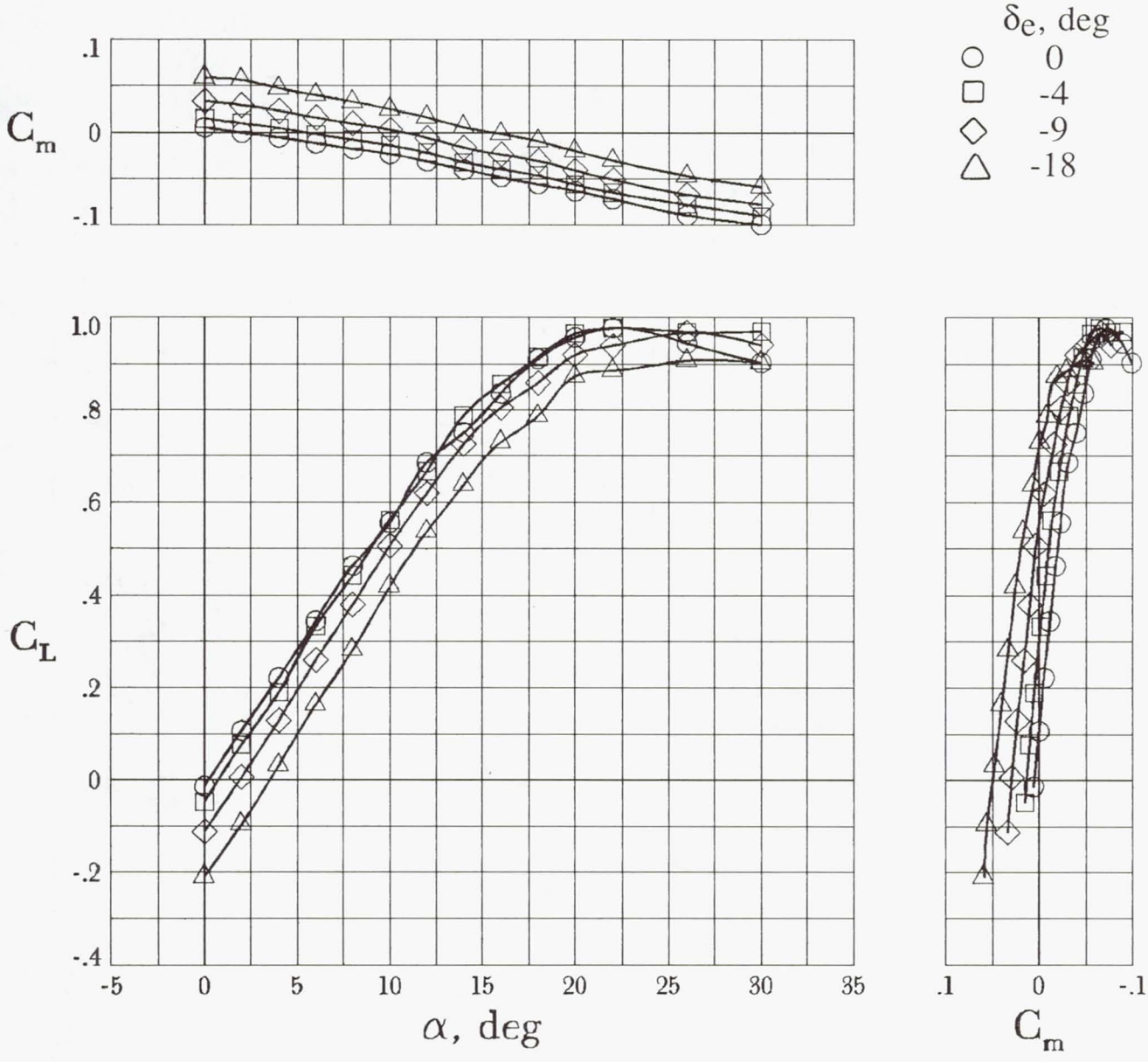

Figure 10. Effect of elevator deflection on the modified Exdrone RPV configuration. Aileron control surfaces preset to $\delta_{a,\mathrm{l}} = \delta_{a,\mathrm{r}} = -4°$.

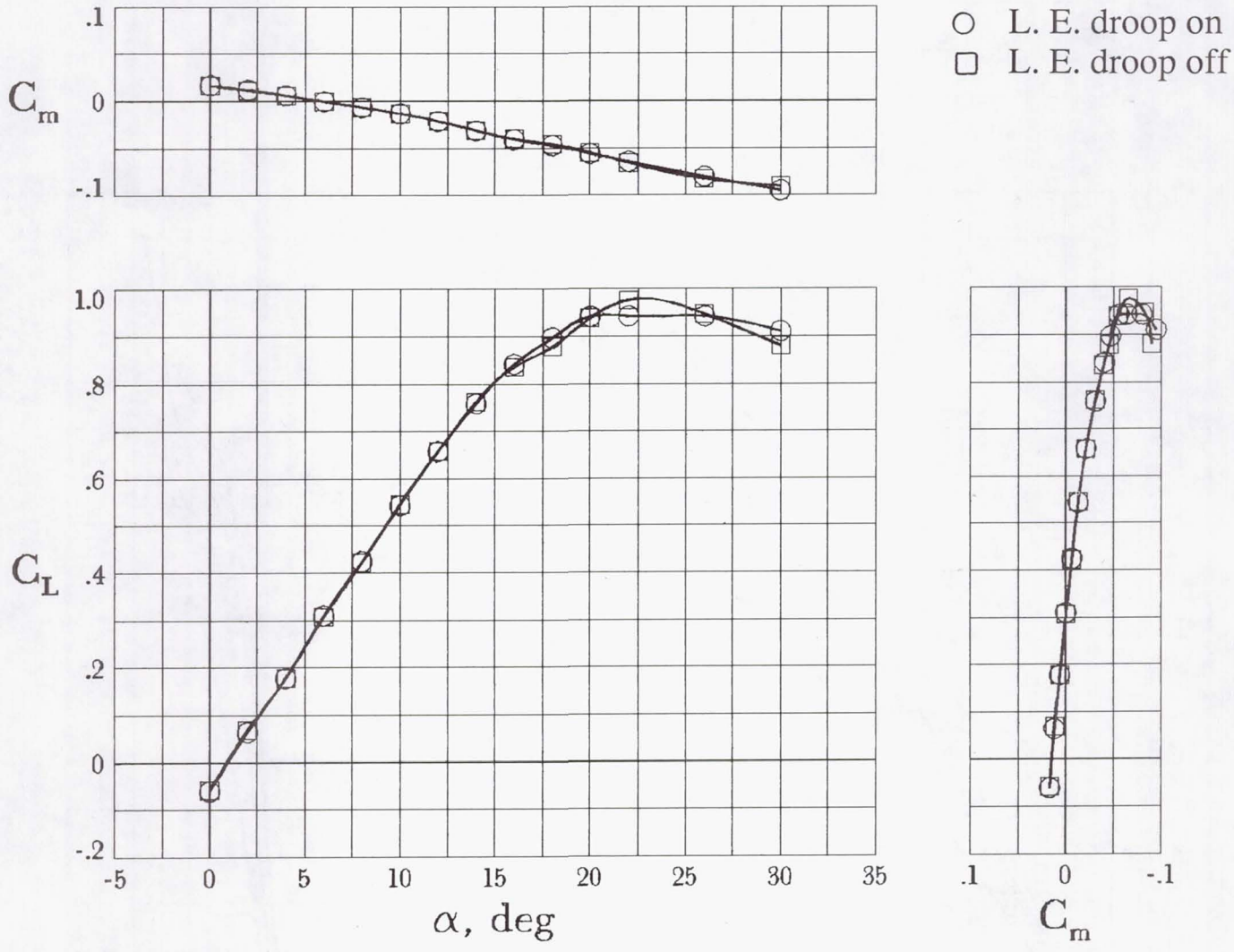

Figure 11. Effect of leading-edge droop modification on the longitudinal aerodynamic characteristics of the modified configuration.

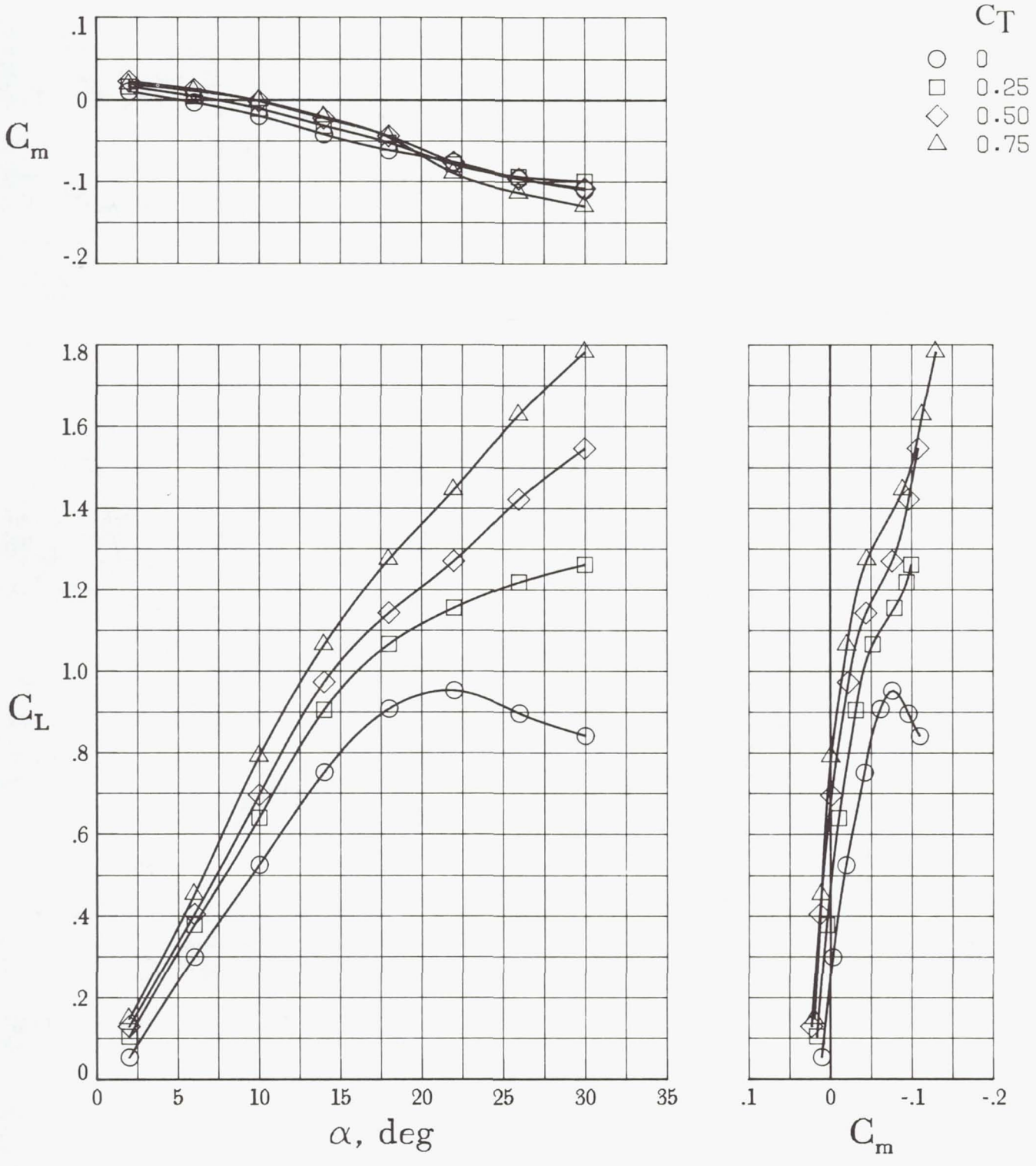

Figure 12. The effect of power on the longitudinal aerodynamic characteristics of the modified configuration.

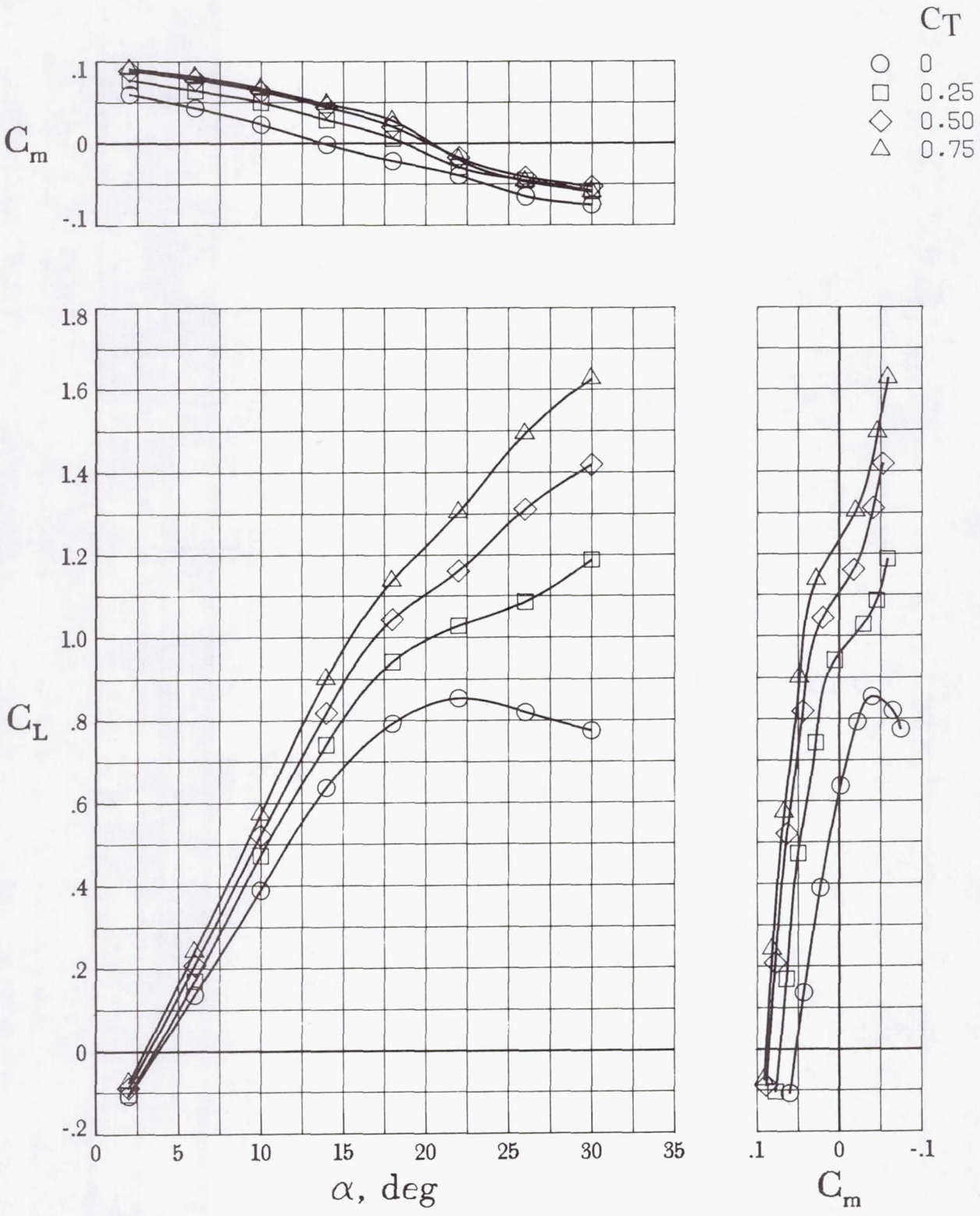

Figure 13. The effect of power on the longitudinal trim of the modified configuration with maximum nose-up pitch control of $\delta_e = -18°$.

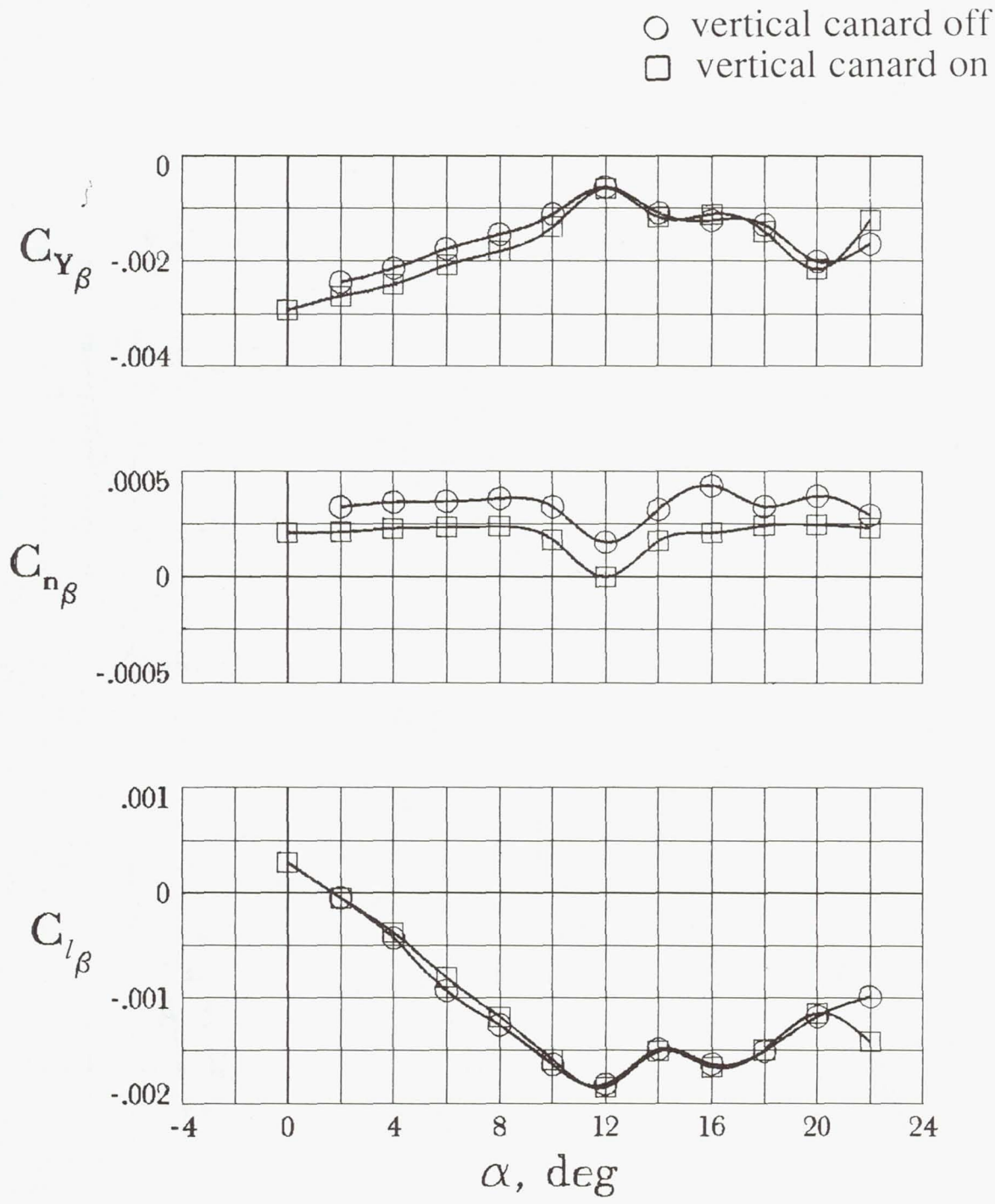

Figure 14. Lateral-directional stability characteristics of the baseline configuration.

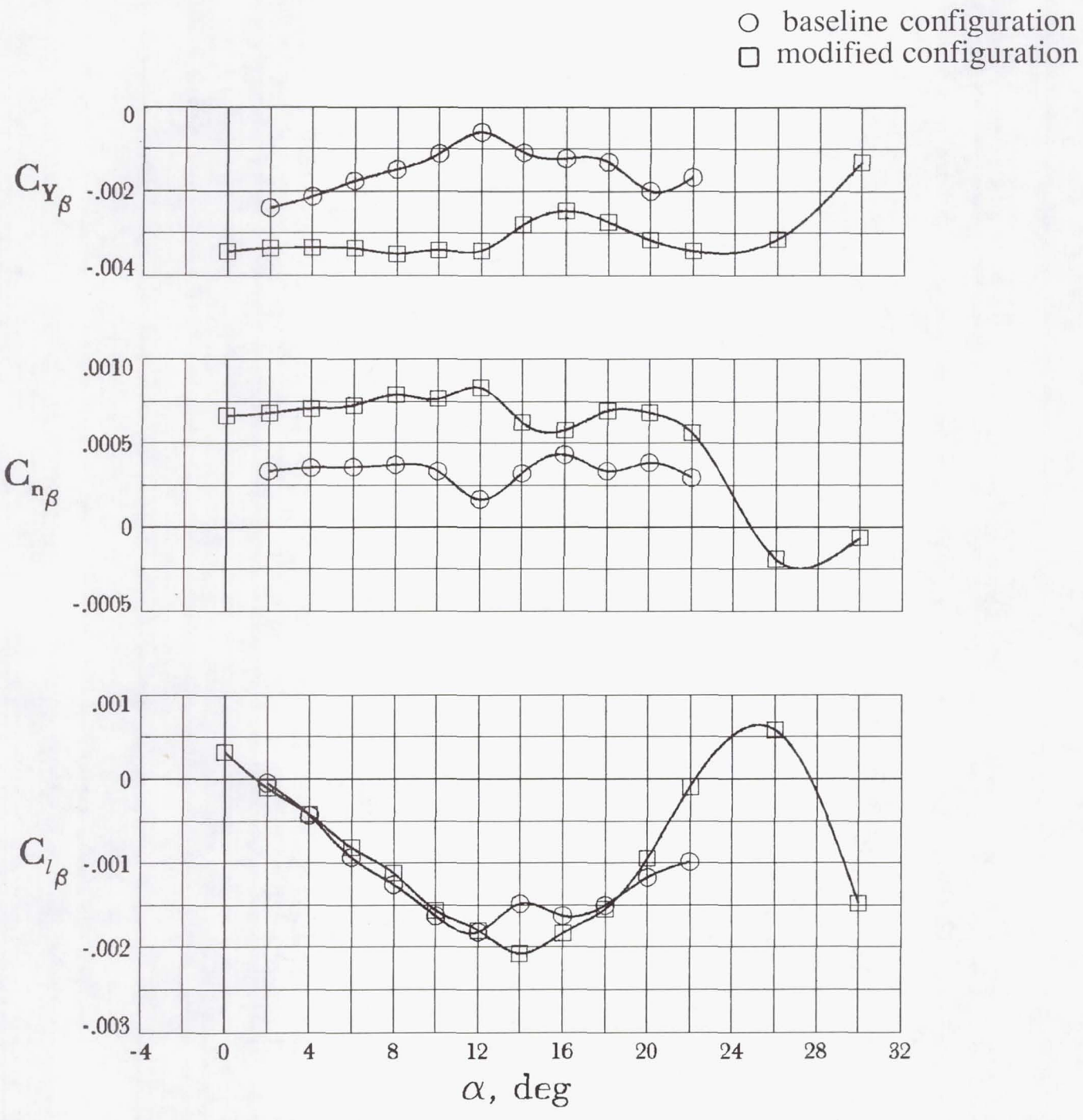

Figure 15. Comparison of the lateral-directional stability characteristics between the baseline and modified configurations.

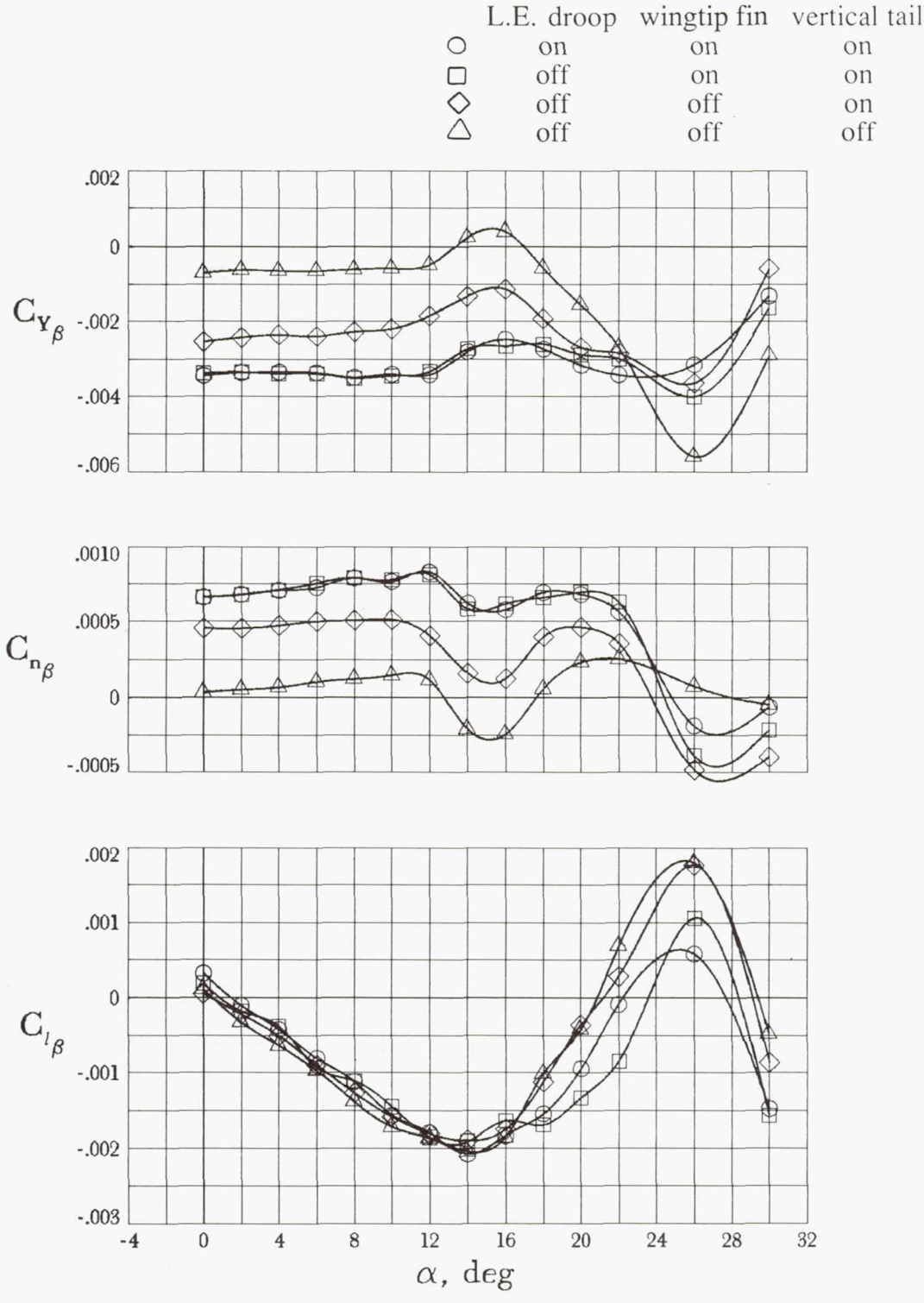

Figure 16. Effect of various configuration components on the lateral-directional stability characteristics of the modified configuration.

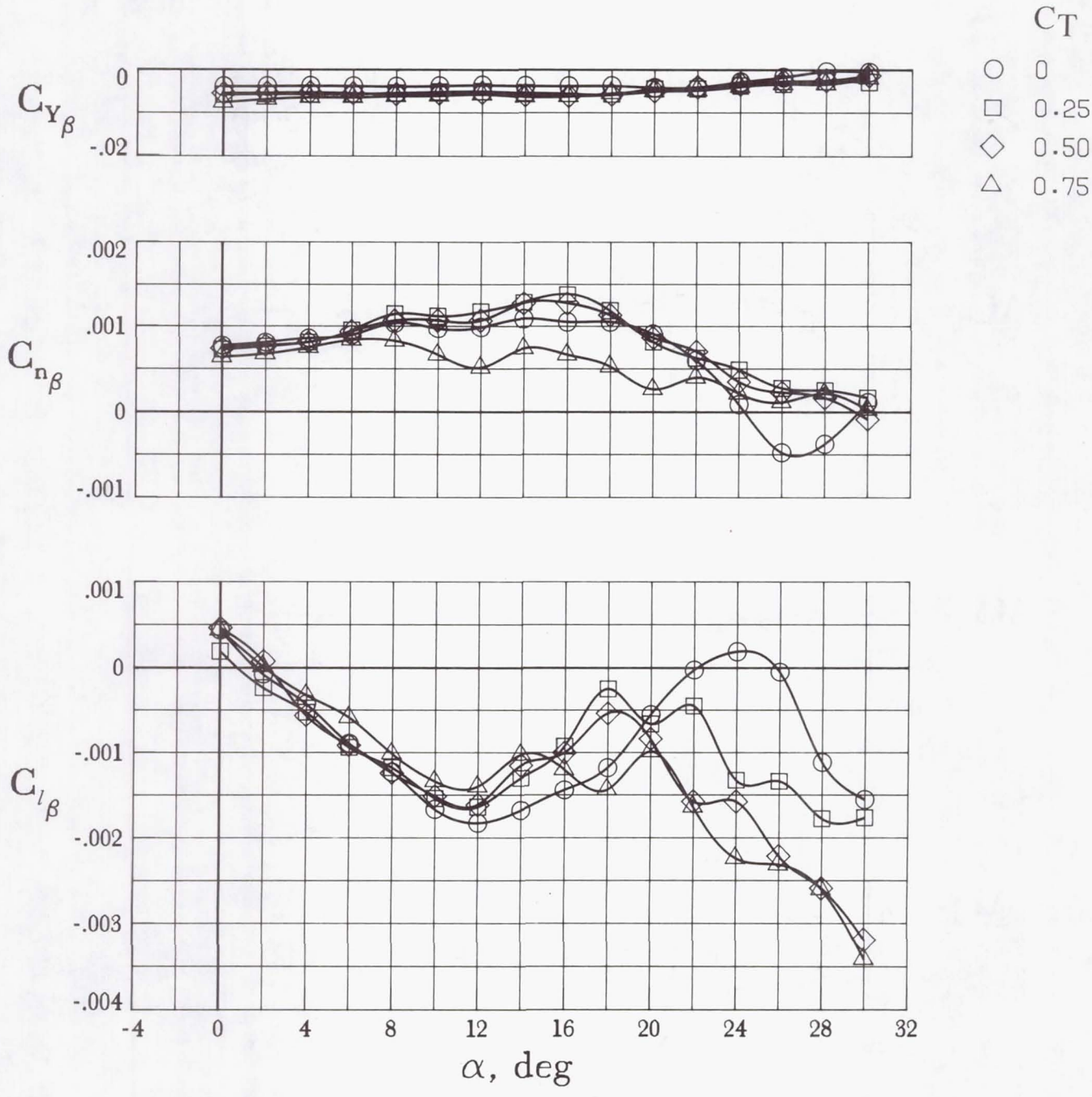

Figure 17. Effect of power on the lateral-directional stability characteristics of the modified configuration.

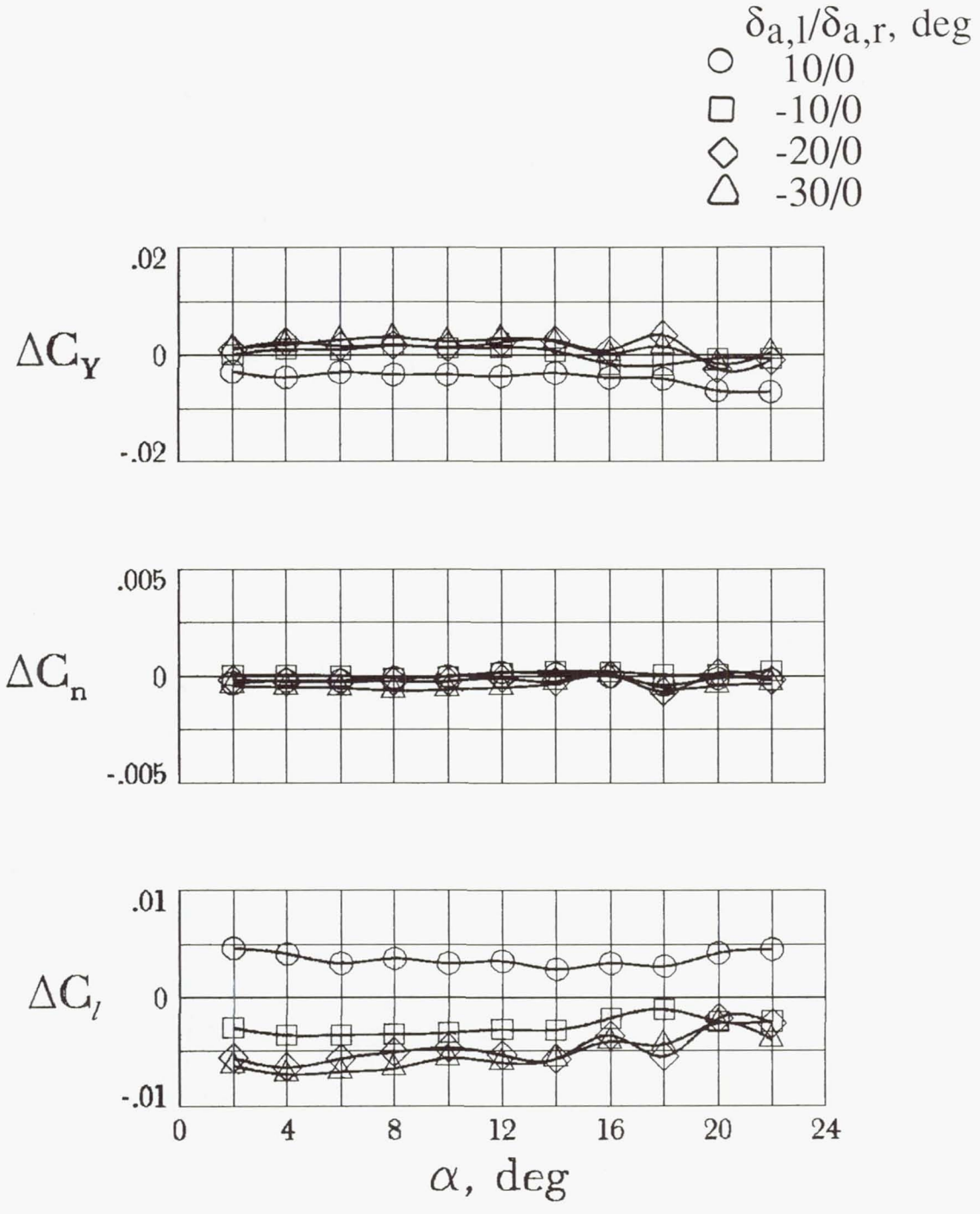

Figure 18. Effect of aileron deflection on the baseline configuration. $C_T = 0$.

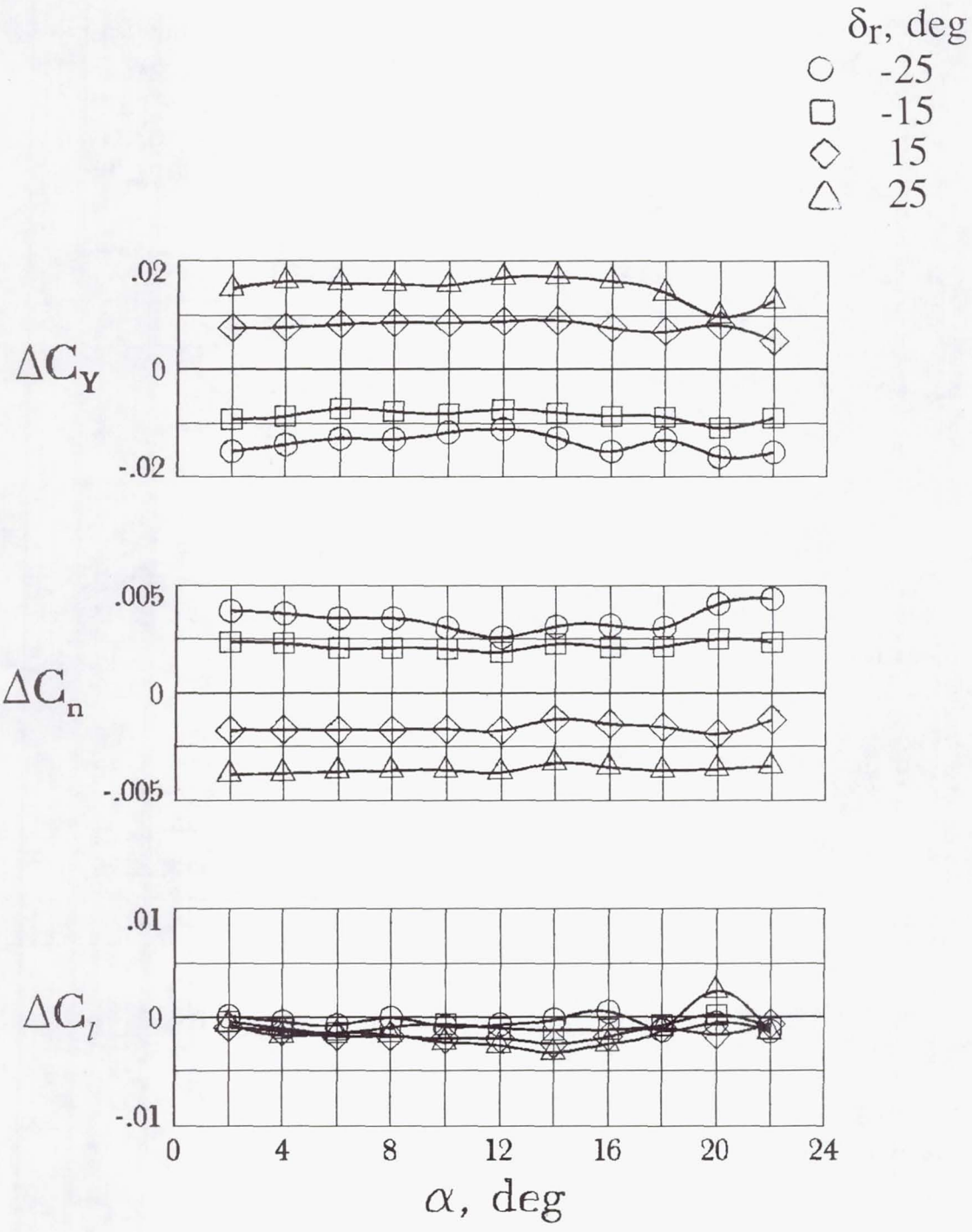

Figure 19. Effect of rudder deflection on the lateral-directional aerodynamic characteristics of the baseline configuration. $C_T = 0$.

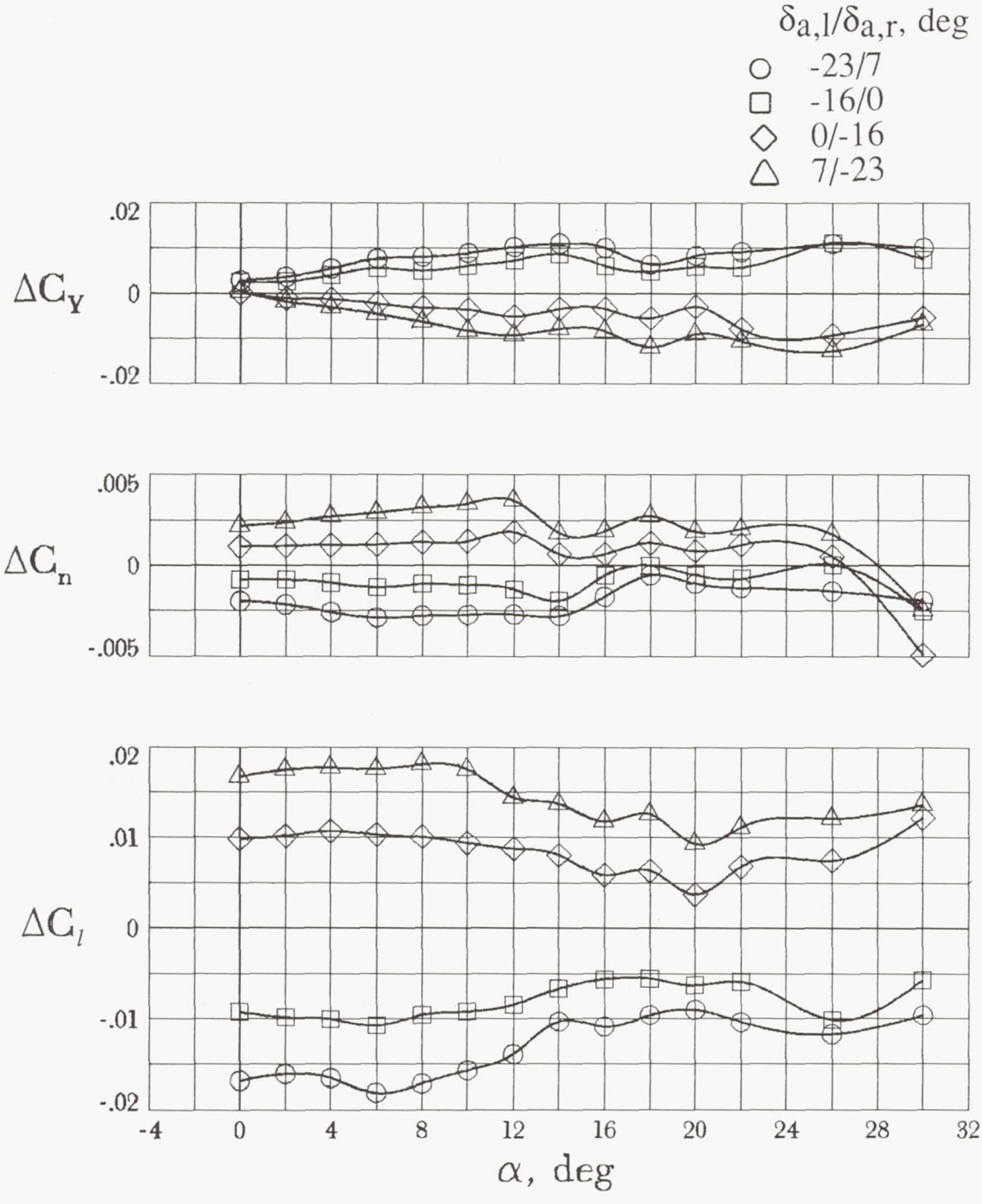

Figure 20. Effect of aileron deflection on roll control for the modified configuration. $\delta_e = -4°$; $C_T = 0$.

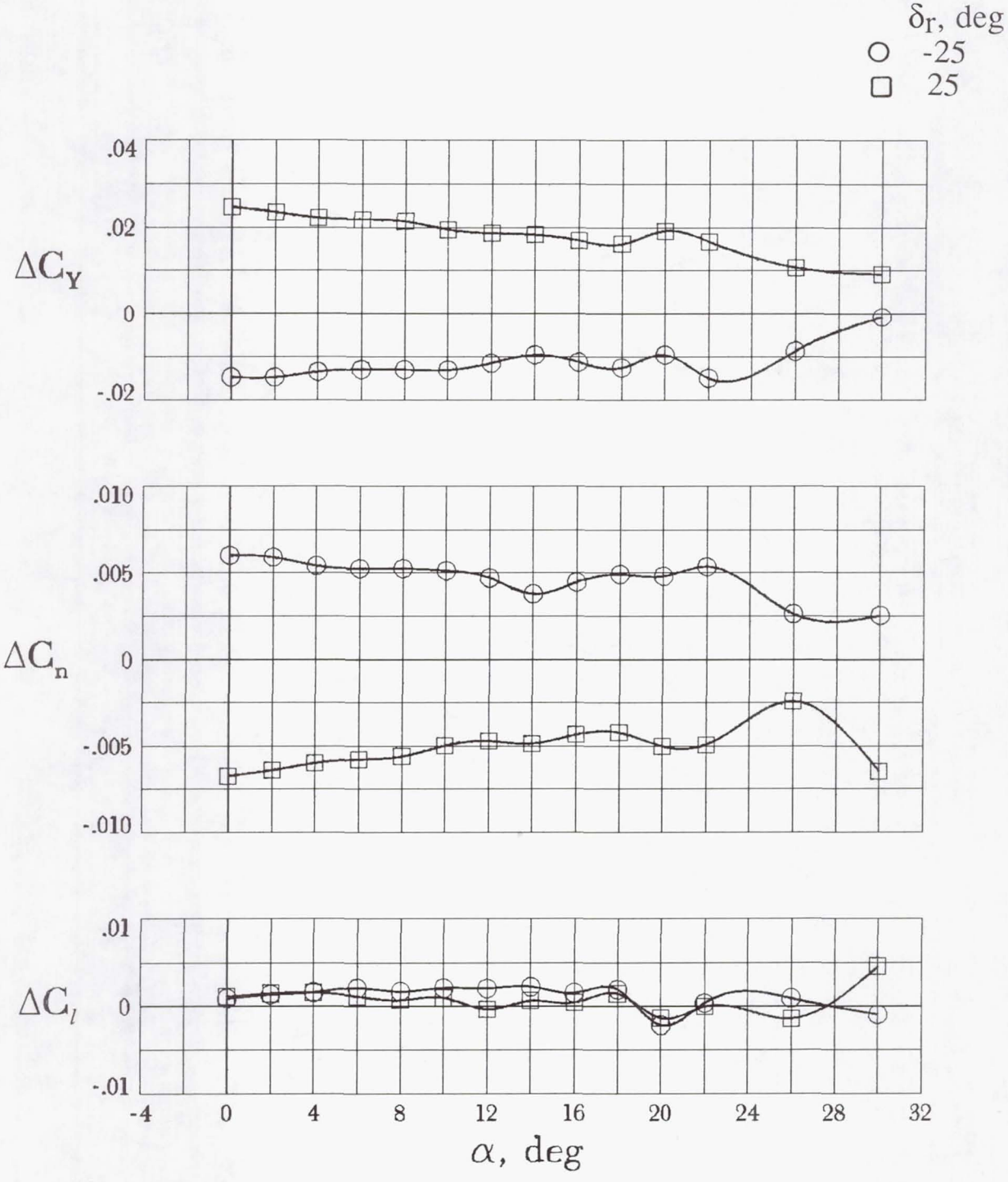

Figure 21. Effect of rudder deflection on yaw control for the modified configuration. $C_T = 0$.

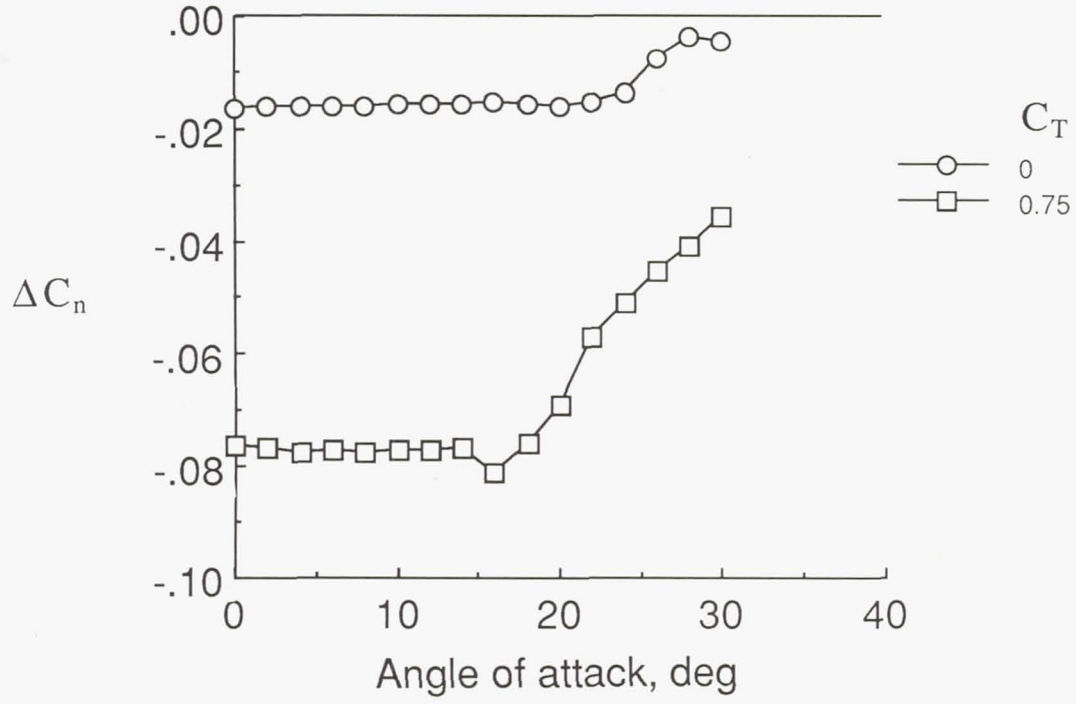

Figure 22. Effect of power on the rudder control authority of the modified configuration. $\delta_r = 25°$.

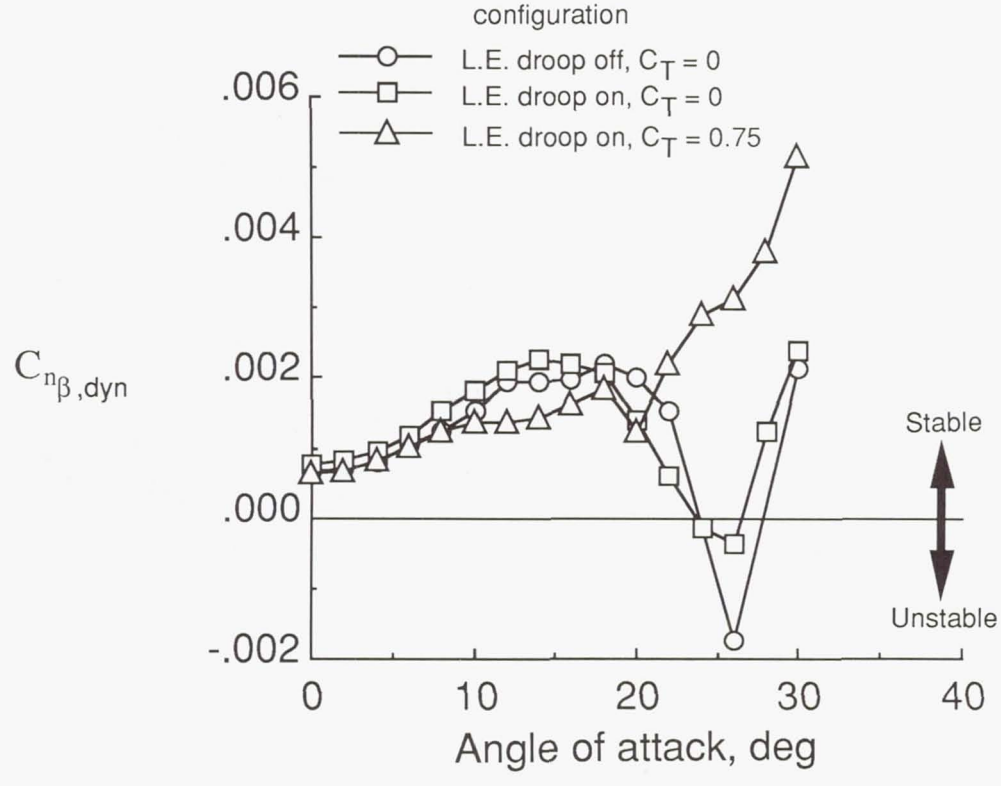

Figure 23. Effect of L.E. droop and power on the yaw divergence parameter $C_{n_{\beta,\mathrm{dyn}}}$ of the modified configuration. Controls neutral.

NASA
National Aeronautics and Space Administration

Report Documentation Page

1. Report No.	2. Government Accession No.	3. Recipient's Catalog No.
NASA TM-4200		

4. Title and Subtitle	5. Report Date
Static Wind-Tunnel and Radio-Controlled Flight Test Investigation of a Remotely Piloted Vehicle Having a Delta Wing Planform	July 1990
	6. Performing Organization Code
7. Author(s)	8. Performing Organization Report No.
Long P. Yip, David J. Fratello, David B. Robelen, and George M. Makowiec	L-16742
9. Performing Organization Name and Address	10. Work Unit No.
NASA Langley Research Center Hampton, VA 23665-5225	505-61-71-69
	11. Contract or Grant No.
12. Sponsoring Agency Name and Address	13. Type of Report and Period Covered
National Aeronautics and Space Administration Washington, DC 20546-0001	Technical Memorandum
	14. Sponsoring Agency Code

15. Supplementary Notes

Long P. Yip, David J. Fratello, and David B. Robelen: Langley Research Center, Hampton, Virginia.
George M. Makowiec: Vigyan Research Associates, Inc., Hampton, Virginia.

16. Abstract

At the request of the U.S. Marine Corps, an exploratory wind-tunnel and flight test investigation was conducted by the Flight Dynamics Branch at the NASA Langley Research Center to improve the stability, controllability, and general flight characteristics of the Marine Corps Exdrone RPV (remotely piloted vehicle) configuration. Static wind-tunnel tests were conducted in the Langley 12-Foot Low-Speed Tunnel to identify and improve the stability and control characteristics of the vehicle. The wind-tunnel test resulted in several configuration modifications, which included increasing the size of the elevator, rudder, and vertical tail; increasing the vertical tail moment arm; adding vertical wingtip fins; and adding leading-edge droops on the outboard wing panel to improve stall departure resistance. Flight tests of the modified configuration were conducted at the NASA Langley Plumtree Test Site to provide a qualitative evaluation of the flight characteristics of the modified configuration.

17. Key Words (Suggested by Authors(s))	18. Distribution Statement
RPV, remotely piloted vehicle UAV, unmanned aerial vehicle Wind-tunnel test Flight test Stability and control Radio-controlled model Stall departure	Unclassified—Unlimited Subject Category 02

19. Security Classif. (of this report)	20. Security Classif. (of this page)	21. No. of Pages	22. Price
Unclassified	Unclassified	33	A03

For sale by the National Technical Information Service, Springfield, Virginia 22161-2171